Journal of Thermal Science Vol.28, No.3 (2019) 394–430

https://doi.org/10.1007/s11630-019-1118-4 **Article ID: 1003-2169(2019)03-0394-37**

Supercritical CO_2: Properties and Technological Applications - A Review

NIKOLAI Polikhronidi[1], RABIYAT Batyrova[1], ASLAN Aliev[1,2], ILMUTDIN Abdulagatov[3,4,*]

1. Thermodynamics of Fluids and Critical Phenomena, Institute of Physics of the Dagestan Scientific Center of the Russian Academy of Sciences, Makhachkala 367003, Dagestan, Russian Federation
2. Mountain Botanical Garden of the Dagestan Scientific Center of the Russian Academy of Sciences, Makhachkala, 367003, Dagestan, Russian Federation
3. Thermophysics Division, Geothermal Research Institute of the Russian Academy of Sciences, Makhachkala 367003, Dagestan, Russian Federation
4. Physical Chemistry Department, Dagestan State University, Makhachkala 367000, Dagestan, Russian Federation

Abstract: The main goal of the present paper is to assess the available information so as to obtain a general procedure for dealing with the critical enhancement of the thermodynamic and transport properties of supercritical CO_2 and CO_2 containing binary mixtures for practical and scientific applications. The present review provides comprehensive analysis of the thermodynamic and transport properties of supercritical carbon dioxide and CO_2 containing binary mixtures (experiment and theory) and their various technological and scientific applications in different natural and industrial processes. The available information for the thermodynamic and transport properties (experiment and theory) enhancement (anomaly) of supercritical carbon dioxide and SC CO_2 + solute mixtures is comprehensively reviewed. The effect of long-range order parameter fluctuations on the thermodynamic and transport properties of supercritical fluids (SC CO_2) will be discussed. Simplified scaling type equation based on mode-coupling theory of critical dynamics with two critical amplitudes and one cutoff wave number as fluid-specific parameters was used to accurately predict of the transport properties of supercritical carbon dioxide. The recommended values of the specific parameters (asymptotic critical amplitudes) of the carbon dioxide for practical (prediction of the thermodynamic and transport properties of the supercritical CO_2 for technological applications) and scientific use were provided. The role of the critical line shapes of the carbon dioxide containing binary mixture (SC CO_2+solvent) in determination of the critical behavior of the mixture near the critical point of pure supercritical solvent (CO_2) is discussed. Krichevskii parameter concept for a description of thermodynamic behavior of dilute near-critical SC CO_2+solute mixtures is also discussed. The structural and thermodynamic properties of the carbon dioxide containing binary mixtures near the critical point of pure solvent (CO_2) are discussed.

Keywords: carbon dioxide, critical point, equation of state, supercritical fluid, thermodynamic properties, transport properties

Received: Nov 15, 2018 Corresponding author: ILMUTDIN Abdulagatov E-mail: ilmutdina@gmail.com

1. Introduction

1.1 Need for thermodynamic properties data for supercritical carbon dioxide

Carbon dioxide is one of the important natural fluids and is widely used in various commercial and industrial applications. During the past years, interest in using CO_2 has increased because of its advantageous thermodynamic and transport properties in supercritical conditions and its environmental impact. Deeply understanding of the properties of supercritical fluids and SC CO_2 containing binary mixtures (SC CO_2+solute) is extremely important from both the fundamental and the technological point views. Supercritical fluids have a large range of potential in the various technological applications. A deeper understanding of the microstructure, thermodynamic and transport properties behavior of supercritical fluids and binary CO_2 containing mixtures near the critical point of pure solvent (SC CO_2) will lead to marked improvements in industrial applications of the supercritical technologies for environmental [1-3], mechanical, chemical, biological, and geothermal industries [4]. The global warming becomes more serious problem due to the increases in atmospheric carbon dioxide. By 2030, CO_2 emission in USA reaches 6.41 billion tones according to the EIA. Green energy use is a good choice. Responding to the need to reduce atmospheric emissions of CO_2, Brown [2] proposed a novel hot dry rock concept that would use CO_2 as heat transmission fluid, and would achieve geologic sequestration of CO_2 as an addition benefit. Heat engines that use supercritical CO_2 as a working fluid can obtain 45 % thermal efficiency and this can be of great benefit to fossil, renewable, and advanced nuclear power plants [5]. Heat engines that use SC CO_2 as a working fluid are smaller and less complex than heat engines that use many traditional working fluids including superheated steam, helium, and organics. Therefore, new studies of the properties of supercritical fluids are of great consequence [5]. Supercritical CO_2 (SC CO_2) has attracted much interest worldwide as a novel heat transmission fluid in recent years [1,2]. The CO_2 has unique feature, in areas with limited water resources using CO_2 as an alternative to water as a working fluid [6]. The thermal siphon power generation and analysis between water and carbon dioxide is presented by Atrens et al. [6]. In 2014, Xu et al. [7] studied fluid and rock chemical interaction in CO_2- EGS (Engineered Geothermal System, energy production). Hsieh et al. [8] discussed the heat transfer phenomena of supercritical CO_2 are experimentally studied in upward flow vertical tube with silica-based porous media. For the availability of CO_2-EGS, researchers have discussed several topics, including CO_2 mineralization by injecting CO_2 into granite and sandstone [9], carbon capture utilization and sequestration [10], geothermal production and CO_2 sequestration in CO_2-EGS [11]. In the works [12-14] have been studied heat transfer phenomena related to CO_2-EGS. The flow rate and pressure are the most important parameters in the EGS. All of these studies have been limited by the lack of an experimental system for investigating the performance of supercritical CO_2 in a reservoir. In this works were shown that efficiency of EGS by using the supercritical CO_2 considerable increases the heat extraction of the silica-based porous media in the experimental scale.

Carbon dioxide capture at supercritical conditions and geologic sequestration is considered as one of the most promising technology to mitigate atmospheric emissions of CO_2 from large-scale fossil fuel usage. The storage of CO_2 at supercritical conditions in deep geologic formations (or geologic CO_2 sequestration technology) is widely considered a feasible approach to reducing industrial loadings of greenhouse gases to the atmosphere [15-19]. Large volumes of CO_2 may be geologically stored by injecting supercritical and thus pressurized CO_2 into saline formations or depleted oil and gas reservoirs [20-22]. One of the conditions which must be met for successful sequestration in formations is temperature and pressure conditions must be such that CO_2 will be supercritical [19]. As well-known, carbon capture and storage technologies are expected to play a key role in strategies to mitigate climate changes, by ensuring large reductions in the rising CO_2 emissions from the continued use of fossil fuels. Key areas like methodologies to identify and assess safe underground storage sites and their monitoring, during and after CO_2 injection or the risks to health, ecosystems and atmosphere due to CO_2 leakages are still poorly known and highly relevant. Furthermore, storing CO_2 deep below the earth's surface or saline aquifers stands as one of the most promising approaches and the knowledge of the CO_2 behavior in the surrounding environment stands as highly relevant to the proper long-term environmental safe storage. It is well–known that the CO_2 sequestration is important and it connects with the global energy and global warming (climate changes) problems. Although CO_2 sequestration plays a vital role in reducing global CO_2 emissions, there is a high risk associated with the process, as the injected CO_2 may back–migrate into the atmosphere sometime after injection. In compare with the other CO_2 sequestration approaches, long-term storage of CO_2 in deep saline aquifers has more advantages and has also been identified as a safe, practical and economically attractive approach to store captured CO_2. This technique is the most technically feasible approach with no negative environmental impacts and have the largest storage capability (up to 10 000 Gt CO_2 could be storied in worldwide aquifers). However, the method has major drawback in compare with other techniques (for example, depleted oil and gas reservoirs and unmineanble coal seams) which is no economic benefits. Therefore, most of the present studies were focused on SC CO_2 sequestration method.

As well-known [23-25], from a technological point of view, supercritical fluids provide an attractive media for chemical reactions. Carbon dioxide at the supercritical condition has unique properties as a reaction medium in its supercritical state [23-25]. Reactions in supercritical CO_2 have been reviewed by Kaupp [23], Savage et al. [24], and Clifford and Bartle [25]. Since compressibility ($K_T \to \infty$) at the critical and supercritical conditions is very large, small changes in pressure is causing substantial changes in density which, in turn, affects diffusivity, viscosity, dielectric, solvation, and other properties. Therefore, CO_2 in supercritical conditions are considerably changing the kinetics and mechanisms of chemical reactions, i.e., one can adjust the reaction environment (e.g., solvent properties) by manipulating temperature and pressure. Therefore, chemical reaction rates can be easily controlled by small changes in T and P. The physical and transport properties of supercritical fluids lie between those of a gas and those of a liquid and may provide a reason to consider supercritical fluids as the reaction media. Thus, accurate thermodynamic and transport properties data for near- and supercritical CO_2 and carbon dioxide containing mixtures are needed for deeply understanding of the microscopic nature of the industrial applications process in supercritical CO_2 and other fundamental scientific and technological applications. Thus, the remarkable anomaly thermodynamic and transport properties of supercritical SC CO_2 (see below, Figs. 4 to 12) make it an unusual and very reactive medium which is very well adapted to many other technological applications such as processing of ceramics, crystal growth, thin film deposition, the extraction of pollutants or additives from dense matrix, etc.

1.2 Technological applications of the CO_2 containing supercritical fluid mixtures

Carbon dioxide has a mild (304.13 K) critical temperature and the critical pressure (7.3773 MPa). It is nonflammable, nontoxic, and especially when used to replace freons and certain organic solvents, environmentally friendly. Moreover, it can be obtained from existing industrial processes without further contribution to the greenhouse effect. Carbon dioxide is fairly miscible with a variety of organic solvents, and is readily recovered after processing owing to its high volatility. It is a small linear molecule and thus diffuses more quickly than bulkier conventional liquid solvents, especially in condensed phases such as polymers. Finally, carbon dioxide is the second least expensive solvent after water. The remarkable anomalous properties of supercritical fluids and fluid mixtures are widely used in industry. Supercritical fluids and fluid mixtures are of fundamental importance in geology and mineralogy (for hydrothermal synthesis), in chemistry, in the oil and gas industries (e.g. in tertiary oil recovery), and for some new separation techniques, especially in supercritical fluid extraction. Carbon dioxide is also commonly used in industrial processes such as the processing of petroleum products and enhancement of viscous oil recovery (in tertiary oil recovery and new separation techniques). Supercritical carbon dioxide has been used also as a miscible flooding agent to miscible displacement of hydrocarbons from underground reservoirs, i.e., can be applied to enhanced oil recovery (EOR). SC CO_2 is widely used to improve the EOR processes. To improve our understanding of the mechanism of the process of miscible displacement of reservoir oils by carbon dioxide injection and control those processes, knowledge of model systems would be helpful. EOR processes can be used to recover trapped heavy oil left in reservoirs after primary and secondary recovery methods. Primary and secondary oil recovery methods produce only 15% to 30% of the original oil in reservoir. SC CO_2 can help to accelerate recovery of heavy hydrocarbons and stimulate fluids from oil and gas reservoirs. SC CO_2 is needed to make EOR economical in harsh environments.

As well-known, most energy in the world is provided by burning oil. Also, the reserves of fossil oil in the world are very limited and reducing rapidly. This leads to the search of new more efficient technologies of the residual heavy oil recovery. The oil price is continuously rising which initiates an interest of the researchers to develop new more efficient enhanced oil recovery technologies. In the petroleum reservoirs, the mixtures of natural gas and crude oil are existing at high temperatures and high pressures. Reservoir-fluids are compositions of thousands of hydrocarbons and a few non-hydrocarbons, such as nitrogen, CO_2, and hydrogen sulfide. The phase behavior (P-T-x phase diagram) of the reservoir mixtures (hydrocarbon+CO_2) under high temperature and pressure (reservoir conditions), and their thermodynamic and transport properties are extremely important for development of the gas condensates production technologies. The phase behavior and thermodynamic properties of the mixtures are function of composition, temperature and pressure (thermodynamic condition of the reservoir mixture). The P-T-x phase diagram of gas-condensate and thermodynamic conditions in oil reservoirs is undergoing complex phase and flow behaviors changes during the depletion of the reservoir (Abbasov and Fataliev [26]). This is related with a loss of the valuable condensate fluid in the reservoir. A deep understanding of the influence of phase behavior and composition changes of the reservoir mixtures during the depletion is required to control and predict the performance of gas condensate reservoir (Katz and Kurata [127], Raghavan and Jones [28]). During the oil and gas production, the reservoir pressure decreases, therefore, the hydrocarbon mixtures composition, volumetric (*PVTx*) properties, and phase behavior (*P-T-x*) are also changing. Gas or liquid injections are also causing the reservoir-fluid composition and properties changing. Near- and supercritical fluids with anomaly properties are continuing widely to be used in industry [30-41], for example, in the oil and gas industries to study retrograde condensation phenomena, enhanced-oil-recovery processes, for some new separation techniques, especially in supercritical fluid extraction, coal conversion, etc. N-decane is one of a typical component of petroleum, and can be used as a good candidate for a model system. Heavy crude oils, entrapped in reservoirs can be recovered by injections of a miscible gas (CO_2 at supercritical condition, for example) at high pressures into the reservoir (Manssori and Savidge [42]). Binary mixture of CO_2+n-decane is of interest in modeling of the enhanced-oil-recovery processes. Carbon dioxide was used as a miscible flooding agent to displace heavy crude oil from a reservoir (lowering of the interfacial tension IFT, low-IFT displacement technique), *i.e.*, miscible displacement of reservoir oil by injection of CO_2 at supercritical conditions. Volumetric (*PVTx*) and phase boundary (*P-T-x*) properties (including VLE data) of CO_2+n-decane binary mixture are needed for simulation of petroleum reservoir conditions and for development of the separation processes technologies. Carbon dioxide mixture with crude heavy oil exhibites liquid phase at temperatures above the critical temperature of CO_2, and can be used as driving gas in low-temperature reservoirs. The residual heavy oil displacement efficiency with SC CO_2 essentially depends on phase behavior generated during the displacement processes, i.e., the details of the (*P-T-x*) phase behavior of CO_2 with heavy crude oil components near the critical point should be known (Orr and Taber [43] and Larsen et al. [44]). Phase behavior (*P-T-x* phase diagram) of the natural reservoir mixtures (complex gas-condensate system) is very similar to those for binary mixtures of CO_2+n-decane. The fundamental thermodynamic behavior of carbon dioxide containing binary mixtures such as CO_2+hydrocarbon near the critical point of pure supercritical solvent CO_2 and near the cricondentherm, cricondenbar, and in the retrograde regions, and some details of the phase behavior are still is less understood. Binary mixture of CO_2+*n*-decane is the key system to develop thermodynamic models for prediction of the properties of natural gas-condensate (Voulgaris et al. [45]). The thermodynamic behavior of the complex multicomponent natural gas mixtures in the reservoirs can be understood by the study of simple key binary mixture such as CO_2+n-decane. The binary systems CO_2+ heavy n-alkane are of interest in enhanced oil recovery technologies (see, for example, Refs. [43-51]). This is the reason why use of supercritical CO_2 as a solvent is rapidly increasing in such important areas as enhanced oil recovery [45-50]. Due to the growing interest in the extraction of viscous crude oils (low volatility compounds of oil) with supercritical CO_2 in tertiary oil recovery and new separation techniques, the thermodynamic properties of CO_2+high n-alkane mixtures are of interest to the petroleum and natural gas industry (Doscher and El-Arabi [47]). In order to improve our understanding of the mechanism of the process of miscible displacement of reservoir heavy oils with supercritical carbon dioxide injection, predict and control those processes, a better knowledge of model systems is very useful. In our previous several publication [51-53] we have reported the volumetric (*PVTx* and phase boundary, *P-T-x* diagram) and calorimetric (C_VVTx) property data of the binary CO_2+n-decane mixture near the critical, supercritical and retrograde condensation regions. In these publications we have provided comprehensive thermodynamic (thermal, caloric, phase boundary, critical curves properties) studies of the binary CO_2+n-decane mixtures in the critical, supercritical and retrograde condensation regions. Previously, we also reported the isochoric heat capacity (C_VVTx) and liquid-gas coexistence curve (T_S, P_S, ρ_S) data of the pure components CO_2 (Abdulagatov et al. [54,55]) and n-decane in the near-critical and supercritical regions. Carbon dioxide is one of the main non-hydrocarbon components of the natural gas. Therefore, knowledge of the critical and supercritical thermodynamic and transport property data for the main key components of the natural gas and oil (reservoir mixtures) such as CO_2+hydrocarbon mixtures has potentially important industrial applications in the petroleum and natural gas engineering, for optimal design of chemical reactors and high-pressure extraction and separation equipments. As is well-known, supercritical CO_2 as a solvent offers many potential advantages over conventional organic solvents [56-59]. Therefore, supercritical CO_2 has the potential to replace harmful organic solvents in industrial applications.

Examples of the applications of supercritical CO_2 in the pharmaceutical industry can be found for controlling particle size [60-65]. The use of supercritical CO_2 for environmental cleanup and associated processing is presently the focus of considerable research attention. Environmental applications of the supercritical CO_2 include regeneration of activate carbon, soil remediation, and clean up of aqueous wastes streams [66-74]. Also, as was mentioned above, use of the supercritical CO_2 as a solvent is rapidly increasing in such important areas as enhanced oil recovery processes [75,76]. The main commercial successes of supercritical CO_2 have been in the food processing industry [77-82]. Over a few 1000 varieties of seeds, roots, leaves, flowers, fruits and barks have been successfully extracted with supercritical CO_2 [83]. Also, supercritical carbon dioxide is widely used as a solvent in supercritical fluid extractions and supercritical fluid chromatography [29-38], and was successfully applied for a number of separation and reaction processes [32,33,38-40].

As well-known, the addition of a polar co-solvent such as acetone and ethanol, for example, to a supercritical CO_2 often leads to an enhancement of the solubility of a solute and improving the selectivity of supercritical CO_2 [84-88]. Alcohols were often used as modifiers for CO_2 in supercritical fluid extraction processes. The use of alcohols (for example methanol and ethanol) as a co-solvent can improve both solubility and selectivity as a powerful separation technique. Small amounts of co-solvents (for example, 3 to 5 mol% of methanol or acetone in SC CO_2), which are referred to as modifiers or entrainers, may be used to modify the polarity and solvent strength of the primary supercritical CO_2 to increase the solubility of solutes and their selectivity, therefore, minimize the operating costs in a extraction processes [89-91]. The co-solvents (basically alcohols, hydrocarbons, acetone, etc.) are commonly polar or non-polar organic compounds which are miscible with supercritical carbon dioxide. The addition of a small amount of co-solvent into a primary supercritical solvent (CO_2) tends to change the critical properties (T_C, P_C, ρ_C) of the resulting solvent mixture (CO_2+co-solvent). It is important to choose the right co-solvent because the mixture critical parameters (T_C and P_C) and phase behavior can be different from those of the primary solvent, affecting the operating conditions. For example, the addition of 4.9 mol% hexane to CO_2 increased the mixture critical temperature by 4% and the critical pressure by 15% [92]. Thus, in order to regulate interactions of the fluid with a specific compound, or to manipulate the critical properties of the mixtures, it is very important to introduce polar or non-polar co-solvents into SC CO_2.

Understanding of the phase behavior and critical curve properties of carbon dioxide containing binary mixtures CO_2+solute can facilitate design and efficient operation of supercritical extraction reactors. Phase equilibrium and critical property data are providing the guidelines for system operation to avoid the problems caused by CO_2+solute binary mixtures which are important in determining the treatability of these materials. The fundamental thermodynamic behavior of CO_2+solvent binary mixtures is not understood well enough to allow supercritical fluid chromatography and supercritical fluid extractions to be conducted without the possibility of encountering serious phase behavior problems. Prediction can result in considerable error for the critical curves of mixture estimation which may lead to inadvertent operation in a two-phase (L-V) region of a phase diagram.

Refrigerants, for example, CH_2F_2 (R32) and R134a can be used to modify (effective modifiers) the properties of CO_2 in supercritical chromatography and supercritical fluid extraction. Even CH_2F_2 might be preferable to modifiers like methanol, since polar modifiers are usually not completely miscible with CO_2, or increase the critical parameters. Furthermore, methanol strongly self-associates, which limits its effectiveness as a co-solvent.

The thermodynamic and transport properties of CO_2 at ambient conditions are very well understood and were improved significantly, while the behavior of CO_2 in the highly compressible conditions (near-critical and supercritical conditions) are less clear and currently still of great scientific and practical interest. Thus, supercritical CO_2 plays a key role in both natural and industrial processes and, as was mentioned earlier, in reducing atmospheric emissions of CO_2. While atmospheric CO_2 are near room temperature, similar CO_2 are present at high temperature and high pressure in deep geological formations (underground reservoirs), and other industrial operations at supercritical conditions. Thus, there is great practical interest in the thermodynamic properties of CO_2 at supercritical condition.

There are other very important industrial applications of SC CO_2. For example, using SC CO_2 instead of water in a closed-loop Hot Dry Rock (HDR) system offers some significant advantages over the original Los Alamos concept (Brown [2]). This new HDR concept would employ a binary-cycle power plant with heat exchange from the hot SC CO_2 to a secondary working fluid for use in a Rankine (vapor) cycle. Thermodynamic analyses showed that SC CO_2, due to its unique supercritical anomaly properties, is nearly as good as water when used for heating mining from a confined HDR reservoir.

From fundamental scientific point view, however, we do not yet have a sufficient understanding of the microscopic nature of the properties (especially structural properties) of supercritical CO_2, which is responsible for their unusual thermodynamic behavior in the near- and supercritical regions. A deeper understanding of the microstructure and physical chemical nature of supercritical CO_2 and SC CO_2 containing fluid mixtures properties will lead to considerable improvements of the important practical applications for environmental, mechanical, chemical, biological, and geothermal industries.

1.3 Scientific applications of the supercritical fluid mixtures

There are also very important theoretical aspects that related with near-critical and supercritical phenomena in systems when one of the components (solvent) is near its critical condition [93,94]. For example, negative or positive divergence of the solute properties such as partial molar properties ($\bar{V}_2^{\infty}, \bar{H}_2^{\infty}, \bar{C}_{P2}^{\infty}$) in the immediate vicinity of the solvent's (CO_2) critical point and path-dependence of the solvent properties in near-critical systems are of great theoretical interest [93-98]. The thermodynamic behavior of near-critical and supercritical CO_2+solute mixtures is also of theoretical interest, for example, to understand the effect of solute molecules on the near- and supercritical behavior of solvent (CO_2) or to examine consequences of the isomorphism principle on the critical behavior of solute+solvent mixtures. The shape of the critical curves (T_C–x, P_C–x and ρ_C–x) for CO_2+solute mixtures is of great interest to the study of the critical phenomena in binary mixtures. The shape of the critical locus is very sensitive to difference in solute's and solvent's molecular size and shape, and specific interactions of the components. The thermodynamic properties of infinite dilute mixtures near the critical point of the solvent (carbon dioxide) are completely determined by the critical lines behavior, namely, initial slopes of the critical curves, i.e., (dT_C/dx) and (dP_C/dx) at $x\to 0$ or through the so called Krichevskii parameter (see below). Thermodynamic behavior of the dilute mixtures, when one of the components (solvent, CO_2) is near the critical point, is extremely important for modeling and prediction of the supercritical fluid technological processes.

Thermodynamic prediction methods which are based on the principle of corresponding states also require accurate knowledge of the critical property data of the pure components (T_C, P_C, ρ_C) and critical lines $T_C(x)$, $P_C(x)$, $\rho_C(x)$ of the mixture. It is apparent that the accuracy of the thermodynamic properties prediction in these methods depends on the uncertainties of the pure components and mixtures critical property data. Accurate knowledge of the critical properties of mixtures is important also in predicting their phase behavior near the critical point. The critical point parameters are the key properties in the construction of phase diagrams as they represent the boundary of the vapor-liquid region (accurate define the location and border of the two- and one-phase regions). Determination of the phase boundaries allows one to estimate retrograde regions and appropriate operating conditions for supercritical fluid extraction processes. One of the main problem in developing of the supercritical fluid phase behavior is the lack of reliable experimental critical properties data for the mixtures. The critical properties (the critical curve data) for mixtures are also needed to develop scaling type (crossover) equation of state Kiselev et al. [99-106], Abdulagatov et al. [107], Anisimov et al. [108], Belyakov et al. [109,110], and Povodyrev et al. [111]. There are various approaches to predict the critical properties of mixtures using the correlations [112,113], but most of them are either restricted in the type of mixture to which they are applicable, or are of poor predictive. Also, the type of the phase diagrams of the CO_2+solute binary mixtures defines by the shape of the critical lines [114]. For example, in the well-known classification of phase diagrams proposed by van Konynenburg and Scott [114], binary mixtures of CO_2 with n-alkanes belong to three different types depending on the shape of critical lines. In this classification scheme [114], the systems CO_2+(C_2 to C_4) are belonging to type-I, and CO_2+n-C_8 is the type-II, while CO_2+n-C_{16} is the type-III. As one can see, this example illustrates the complexity that can be observed experimentally for these types binary mixtures.

Thermodynamic and transport property data of near- and supercritical CO_2, such as asymptotic critical amplitudes of isochoric heat capacity ($A_0^{\pm}$) and liquid+gas coexistence curve near the critical point (B_0) and their universal ratios, A_0^{+}/A_0^{-}, $A_0^{+}\Gamma_0^{+}B_0^{2}$, $\alpha A_0^{+}\Gamma_0^{+}B_0^{-2}$, $D_0\Gamma_0^{+}B_0^{\delta-1}$, $\xi_0\left(\dfrac{\alpha A_0^{+}}{v_C}\right)$, with the amplitudes for other properties (compressibility Γ_0^{+}, pressure D_0, and correlation radius ξ_0), are very useful for theory to check and confirm the predictive capability of the existing scaling theory of critical phenomena [115-120] and its physical bases. The critical amplitudes of isochoric heat capacity ($A_0^{\pm}$) and the density on the liquid-gas coexistence curve (B_0) are also defining other very important theoretically meaning critical amplitudes such as $\Gamma_0^{+}=0.058B_0^{2}/\alpha A_0^{+}$, $D_0= 1.69/\Gamma_0^{+}B_0^{\delta-1}$ and $\xi_0^{+}=0.266\left(v_C/\alpha A_0^{+}\right)^{1/3}$ [121] using universal relations between the critical amplitudes. Experimentally determined asymptotical critical amplitudes ($A_0^{\pm}$ and B_0, fluid-specific parameters) of CO_2 can be used to check and confirm the predicted capability of the universal correlations between the asymptotic critical amplitudes and acentric factor ω based on the corresponding states principle [121]. Thus, the main goal of the present review is firstly to give the readers a prospective of supercritical CO_2 applications to thermal and energy sciences (environmental, mechanical, chemical, biological, and geothermal industries), secondly to try to overview the most recent developments in the thermodynamic, transport and structural properties of pure supercritical CO_2 and related CO_2 containing binary mixtures near the critical point of pure solvent (carbon dioxide). In addition, we have reviewed wide-ranging theoretically based (scaling-type) correlations for transport properties and crossover equations of state for CO_2.

2. Effect of Critical Fluctuations on the Thermodynamic and Transport Properties of Supercritical Carbon Dioxide

As well-known, systems near the critical point and in the supercritical region exhibit long-range fluctuations in the order parameter (density difference, $\Delta\rho=\rho-\rho_c$) associated with the phase transition [122]. The fluctuations are characterized by the length (correlation radius ξ) which is diverging at the critical point. Fig. 1 demonstrates the temperature and density dependence of the correlation radius for CO_2 calculated from the fundamental reference equation of state [123,124] for selected supercritical isotherms. These critical fluctuations not only cause critical anomaly of the thermodynamic and transport properties in the immediate vicinity of the critical point, but also affect these properties in a wide range of temperature and pressure around the critical point (supercritical region, see Figs. 2 and 3). These temperature and pressure ranges around the critical point are including the regions where supercritical fluid technology is applicable.

2.1 Thermodynamic properties

The critical anomaly of thermodynamic properties of near- and supercritical fluids is significant over a wide range of density and temperature around the critical point (see Figs. 2 and 3).The literature search based on the TRC/NIST Archive [125] showed that thermodynamic and transport properties of carbon dioxide were well studied by many authors, although there are restricted data in the supercritical conditions. Existing data (TRC/NIST DataBase) cover a wide range of temperature and pressure. 29, 15, 9, and 7 data sources were found in the NIST SOURCE Data Archive for the *PVT*, C_P, C_V, and speed of sound, respectively, at supercritical conditions for carbon dioxide. Also, 19 and 13 data sources are listed in the NIST SOURCE Data Archive for thermal conductivity and viscosity of CO_2, respectively, in the supercritical region. Most reliable and accurate thermodynamic [126-138] and transport [139-147] property data were published in these works. These data were used to develop reference fundamental equations of state [123,148] and reference correlation equations for thermal conductivity [149] and viscosity [150-152] (see also REFPROP [124]). The uncertainties of the reference equation of state [123] for CO_2 are approximately 0.2% (to 0.5% at high pressures) in density, 1% (in the vapor phase) to 2% in heat capacity, 1% (in the vapor phase) to 2% in the speed of sound, and 0.2% in vapor pressure, except in the critical region. The estimated uncertainties of the equation of state reported in Ref. [148] at pressures up to 30 MPa and temperatures up to 523 K range from 0.03% to 0.05% in density, 0.03% (in the vapor) to 1% in the speed of sound (0.5% in the liquid) and 0.15% (in the vapor) to 1.5% (in the liquid) in heat capacity. In this equation of state the special interest has been focused on

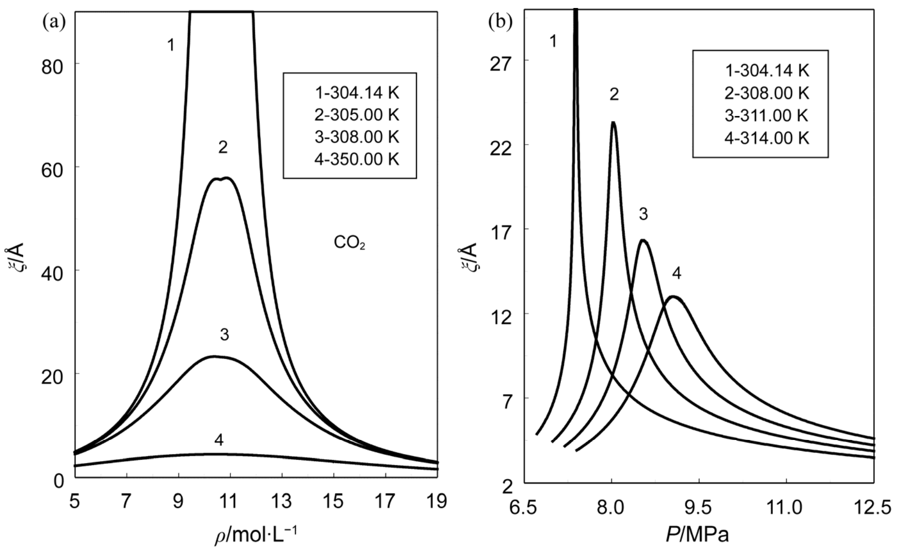

Fig. 1 Correlation radius of CO_2 as a function of density (a) and pressure (b) along the supercritical isotherms calculated from reference EOS by Span and Wagner [123] (REFPROP [124].

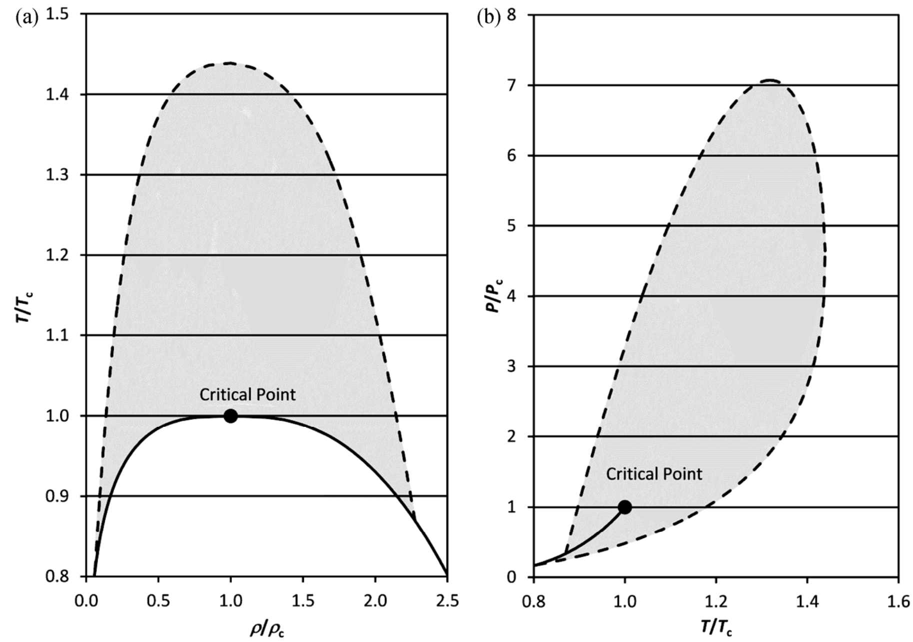

Fig. 2 Reduced ranges of density (ρ), temperature (T), and pressure (P), relative to their values ρ_c, T_c, P_c at the critical point, where the critical enhancement contribution (density fluctuations affects) to the thermodynamic properties is larger than 1% for CO_2. The critical enhancement exceeds 1% in the shaded regions between the saturation curves (solid) and the 1% enhancement curves (dashed).

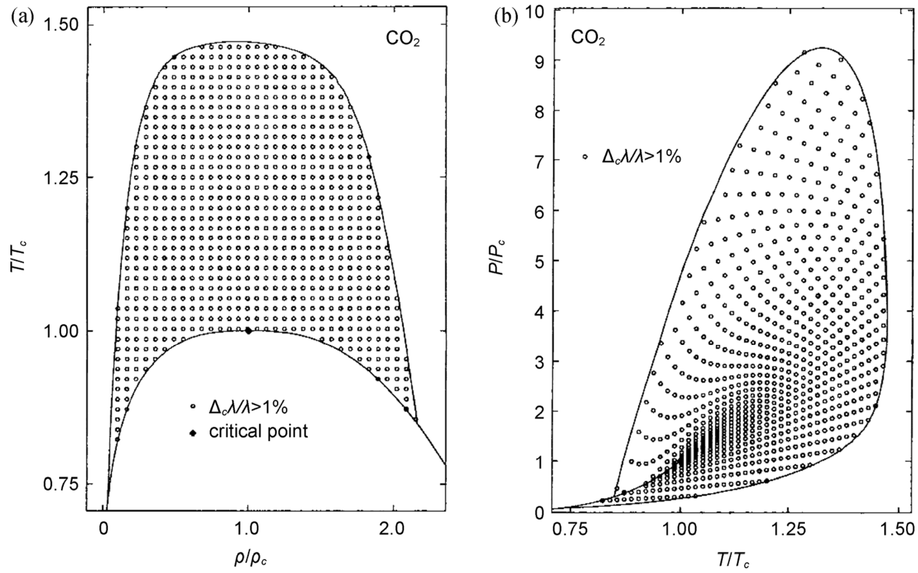

Fig. 3 Contribution of critical enhancement for supercritical CO_2. Reduced ranges of density (ρ), temperature (T), and pressure (P), relative to their values ρ_c, T_c, P_c at the critical point, where the critical enhancement contribution to the thermal conductivity is larger than 1 % for CO_2 [121].

the description of the critical region and the extrapolation behavior of the formulation (to the limits of chemical stability). The overall uncertainty (at the 95% confidence level) of the proposed correlation [149] for thermal conductivity of CO_2 varies depending on the state point from a low of 1% at very low pressures below 0.1 MPa between 300 and 700 K, to 5% at the higher pressures of the range of validity. The uncertainty in viscosity calculated from Refs. [150-152] ranges from 0.3% in the dilute gas near room temperature to 5% at the highest pressures. Reported experimental thermodynamic properties data of supercritical CO_2 together with the values calculated from reference equation of state are shown in Figs. 4 to 9 as a function of pressure and density. As one can see, in general the agreement between the measured and calculated values of thermodynamic properties CO_2 in the supercritical region is good. However, these reference fundamental equations of state are analytical at the critical point (multiparametric equations of state) and incorrectly representing scaling features of anomaly of the thermodynamic functions in the immediate vicinity of the critical point (in the asymptotical region). This means that the equations of state remain analytic at the critical point and do not account the well-known and theoretically confirmed (scaling theory [162-164]) singular behavior of thermodynamic properties in the immediate vicinity of the critical point. For practical applications, we need to calculate thermodynamic properties close to the critical point (including supercritical condition, see Figs. 2 and 3) as well as far away from the critical point where classical (analytic) equations of state is valid. Crossover models are incorporating (smoothly transforming scaling-type EOS to classical mean filed EOS) scaling and classical type equations of state. Crossover scaling type equations of state for CO_2 were developed by Sengers et al. [122,165,166] and Kiselev et al. [153-157,167]. Crossover models [122,153-157,165-167] are incorporating non-analytical scaling laws in the critical region and the analytical (classical mean-field) equation of state far

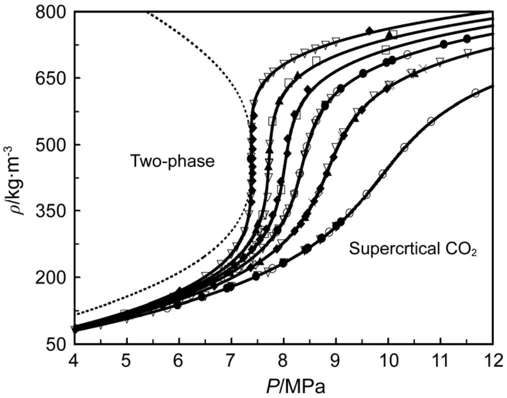

Fig. 4 Measured and calculated densities of carbon dioxide as a function of pressure in the supercritical region. Symbols are reported data from NIST/TRC DATA BASE [125]; Solid lines are calculated from reference equation of state by Span and Wagner [123] (REFPROP [124]); Dashed curve is liquid+gas coexistence boundary [124].

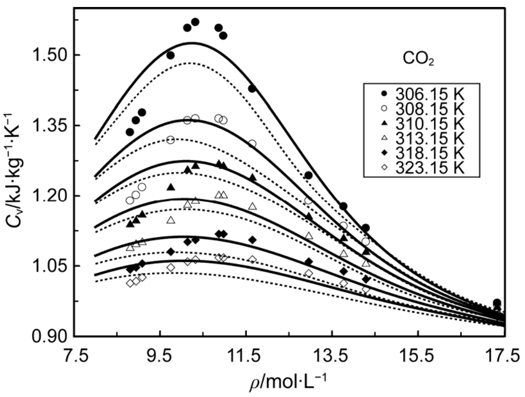

Fig. 5 Measured and calculated isochoric heat capacities of carbon dioxide as a function of density in the supercritical region. Symbols are reported by Amirkhanov et al. [130,131] and Abdulagatov et al. [54,55]; Solid lines are calculated from crossover model [153-157]; Dashed lines are calculated from reference EOS by Span and Wagner [123] (REFPROP [124]).

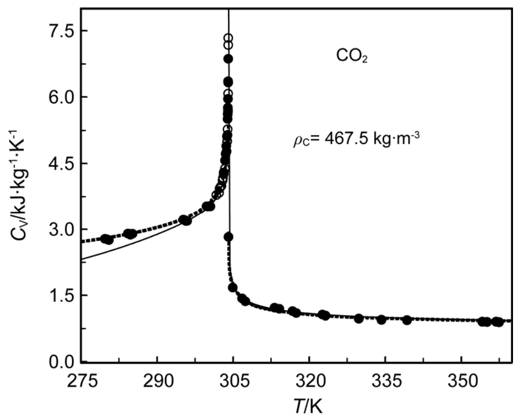

Fig. 6 Measured and calculated isochoric heat capacities of carbon dioxide as a function of temperature along the critical isochore. Solid curve is calculated from crossover model [102,153-157]; • - Abdulagatov et al. [54,55]; ○-Adamov et al. [158,159]; Dashed lines are calculated from reference EOS by Span and Wagner [123] (REFPROP [124]).

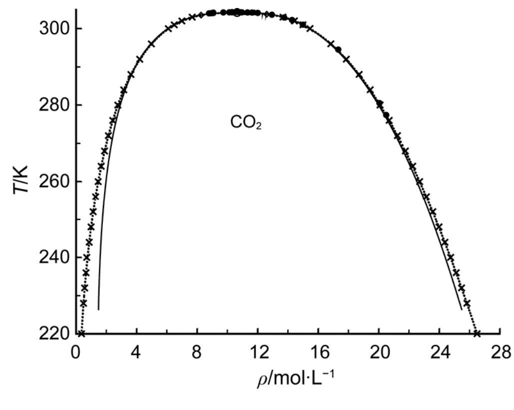

Fig. 7 Saturated densities of carbon dioxide derived from isochoric heat capacity measurements together with the data reported by other author's and calculated from equations of state. •- Amirkhanov et al. [130,131]; Δ- Abdulagatov et al. [54,55]; Other symbols are from NIST/TRC DATA BASE [125]; Solid curve is calculated from crossover model [102,153-157]; Dotted curve is calculated from Span and Wagner [123] (REFPROP [124]).

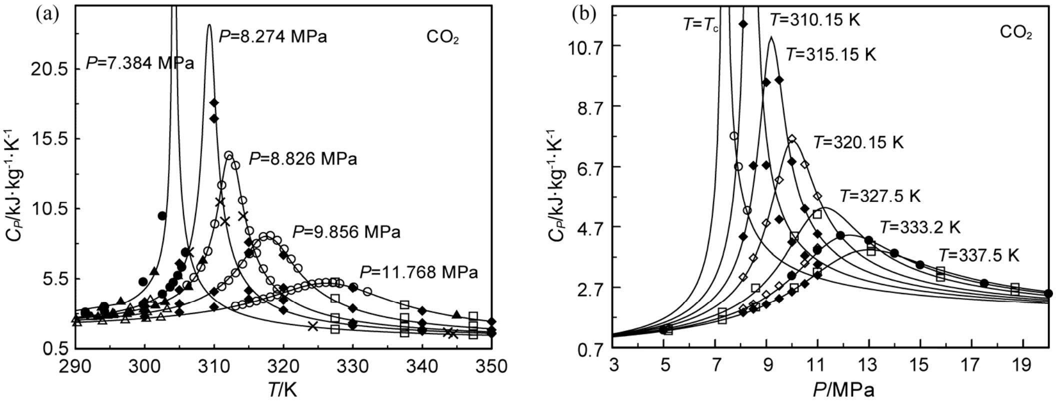

Fig. 8 Measured and calculated isobaric heat capacities of carbon dioxide along the supercritical isobars (a) and supercritical isotherms (b). Symbols are reported data from NIST/TRC DATA BASE [125]; Solid curves are calculated from reference EOS by Span and Wagner [123] (REFPROP [124]).

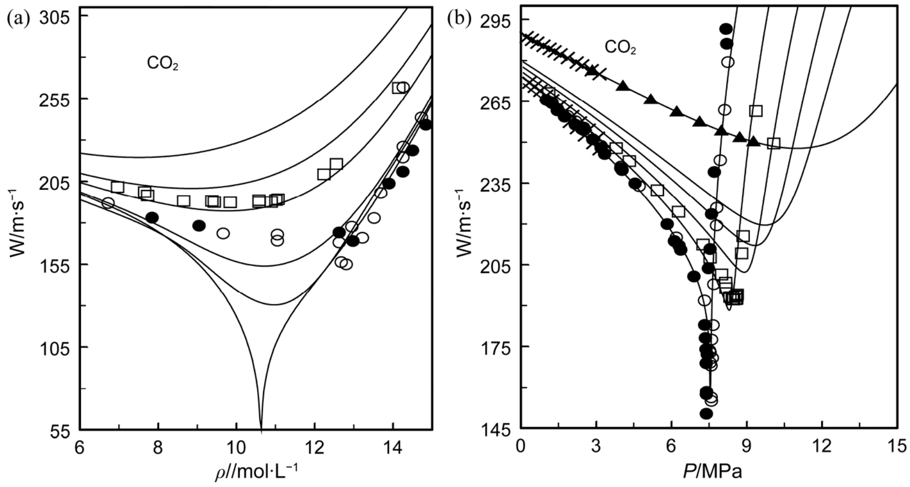

Fig. 9 Measured and calculated speed of sound for carbon dioxide along the supercritical isobars (a) and supercritical isotherms (b) calculated from reference EOS by Span and Wagner [123] (REFPROP [124]). Symbols are reported data by Herget [160] and Estrada-Alexandersa and Trusler [161].

from the critical point. This type equation of state reproduces the thermodynamic properties of supercritical fluids with high accuracy, including the asymptotical scaling behavior and contains minimum adjustable fitting parameters.

2.2 Transport properties

2.2.1 Thermal conductivity of supercritical CO_2

The critical thermal conductivity enhancement is significant over a substantial range of densities and temperatures around the critical point. This phenomenon for thermal conductivity of CO_2 is illustrated in Fig. 3, which shows the reduced ranges of density, temperature, and pressure where the critical enhancement contributes more than 1% to the actual thermal conductivity for CO_2. It is seen that the enhancement is significant over the reduced density range $0.06<\rho/\rho_C<2.27$ and over the reduced temperature range $0.81<T/T_C<1.44$. As one can see from Fig. 3, the thermal conductivity exhibits a considerable increase in the vicinity of their liquid –gas critical points (in the supercritical region). In order to account the effect of the critical fluctuation the total experimentally observed thermal conductivity λ was presented as the sum of an enhancement part $\Delta_C\lambda$ caused by the long-range critical density fluctuations and a background term λ_b which is the thermal conductivity to be expected in the absence of critical fluctuations:

$$\lambda = \Delta_c\lambda + \lambda_b \tag{1}$$

The rate of the critical fluctuations decay in fluids near the liquid-gas critical point is determined by the thermal diffusivity, $D_T=\lambda/\rho C_P$. The separation, Eq. (1), of the thermal conductivity into a critical and a background contribution leads to splitting of the thermal diffusivity D into a critical $\Delta_C D_T= \Delta_C\lambda/\rho C_P$ and a background

$D_b=\lambda_b/\rho C_P$ contributions as $D_T=\Delta_C D_T+D_b$. According to the mode-coupling theory of dynamics critical phenomena, a set of coupled integral equations for the critical contributions to the thermal diffusivity $\Delta_c D(q)$ and the shear viscosity $\Delta_c\eta(q)$ can be used. The dependence of $\Delta_c D(q)$ and $\Delta_c\eta(q)$ on the wave number q of the fluctuations needs to account due to the long-range nature of the critical fluctuations. One then obtains [121]

$$\Delta_c D(q)=\frac{\Delta_c\lambda(q)}{\rho C_P(q)}=\frac{k_B T}{(2\pi)^3\rho}\int_0^{q_D} d\mathbf{k}\left[\frac{C_P(|\mathbf{q}-\mathbf{k}|)}{C_P(q)}\right]\frac{\sin^2\theta}{k^2\eta(k)/\rho+|\mathbf{q}-\mathbf{k}|^2 D(|\mathbf{q}-\mathbf{k}|)} \tag{2}$$

$$\Delta_c\eta(q)=\frac{1}{2q^2}\frac{k_B T}{(2\pi)^3}\int_0^{q_D} d\mathbf{k}\, C_P(k)C_P(|\mathbf{q}-\mathbf{k}|)\left[\frac{1}{C_P(k)}-\frac{1}{C_P(|\mathbf{q}-\mathbf{k}|)}\right]^2\frac{k^2\sin^2\theta\sin^2\phi}{k^2 D(k)+|\mathbf{q}-\mathbf{k}|^2 D(|\mathbf{q}-\mathbf{k}|)} \tag{3}$$

where k_B is Boltzmann's constant and T the temperature, and θ and ϕ are the azimuthal and polar angles of the wave vector $\mathbf{k}$ with respect to the wave vector $\mathbf{q}$. The integrals in Eqs. (2) and (3) are to be evaluated over all values of $k=|\mathbf{k}|$ up to a maximum value of q_D. The maximum value of q_D corresponds to a length of scale separating long- and short-range critical fluctuations. As one can see, D, η, and C_P depend only on the value of the critical fluctuations wave vector. In order to deduce the critical contributions to the thermal diffusivity, thermal conductivity, and shear viscosity, we need the solution of Eqs. (2) and (3) in the hydrodynamic limit $q\to 0$.

In the asymptotical range of the critical point $\Delta_C D_T$ approaches a Stokes-Einstein law $\Delta_c D=\Delta_c D(0)\approx\frac{R_D k_B T}{6\pi\eta\xi}$, where ξ is a correlation length and R_D universal dynamic amplitudes ratio. In the asymptotical range of the critical point the viscosity η obeys to the simple power law $\eta\approx\eta_b(Q\xi)^z$, where $z=8/15\pi^2=0.054$ is a universal dynamic critical exponent and where Q is a system-specific coefficient. The contribution of the fluctuation term of the viscosity is very small, therefore it can be neglected for practical applications. Hence, $\eta(k)$ in Eq. (2) can be replace by $\eta\approx\eta_b$ as an independent of the wave number k. In the limit $q\to 0$ Eq. (2) reduces to [121]

$$\Delta_C D=\frac{\Delta_C\lambda}{\rho C_P}=\frac{R_D k_B T}{(2\pi)^3\eta}\int_0^{q_D} d\mathbf{k}\left[\frac{C_p(k)}{C_P(0)}\right]\frac{k^{-2}\sin^2\theta}{1+\rho D(k)/\eta} \tag{4}$$

In Eq. (4) we included the universal dynamic amplitude R_D, therefore, Eq. (4) will reproduce the asymptotic critical behavior of $\Delta_C D$ near the critical point. In the immediate vicinity of the critical point the term $\rho D(k)/\eta$ in Eq. (4) becomes negligibly small, since the thermal diffusivity $D\to 0$ vanishes at the critical point, while far away from the critical point the contribution of $\rho D(k)/\eta$ is positive. Therefore, neglecting of this term leads to overestimating of the integral value. The contribution of this term never becomes large. To compensate of the overestimation we need to integrate up to a lower cutoff wave number $\bar{q}_D<q_D$

$$\Delta_C D=\frac{\Delta_C\lambda}{\rho C_P}=\frac{R_D k_B T}{(2\pi)^3\eta}\int_0^{\bar{q}_D} d\mathbf{k}\left[\frac{C_p(k)}{C_P(0)}\right]\frac{\sin^2\theta}{k^2} \tag{5}$$

As one can note Eq. (4) is identical to the mode-coupling integral considered by Kawasaki [168] and Ferrell [169], difference in the presence of a finite upper cutoff wave number $\bar{q}_D$. A finite upper cutoff number is necessary for getting a physically correct nonasymptotic critical behavior of the thermal conductivity.

Using the approximations reported by Olchowy and Sengers [170], representation of the critical enhancement can be written as

$$\Delta_C\lambda=\rho C_P\Delta_C D=\frac{\rho C_P R_D k_B T}{6\pi\eta\xi}Y(\bar{q}_D\xi) \tag{6}$$

where Y is a crossover function defined by

$$Y(y)\equiv\frac{2}{\pi}\left\{\left[\left(1-\kappa^{-1}\right)\arctan(y)+\kappa^{-1}y-\left[1-\exp\left(\frac{-1}{y^{-1}+y^2\rho_c^2/3\rho^2}\right)\right]\right]\right\} \tag{7}$$

κ is the ratio $\kappa=\frac{C_P}{C_V}$. At the $y=\bar{q}_D\xi\to\infty$, Eq. (6) represents the asymptotic critical behavior as $\Delta_c D=\Delta_c D(0)\approx\frac{R_D k_B T}{6\pi\eta\xi}$. Since mode coupling accounts presence of the long-time-tail contributions to the transport properties far from the critical point in the background thermal conductivity λ_b, the mode-coupling integrals (2) and (3) are not vanishing in the range far from the critical point. However, the critical part of the thermal conductivity will vanish at $y=\bar{q}_D\xi\to 0$ far from the critical point, since the second term in Eq. (7)

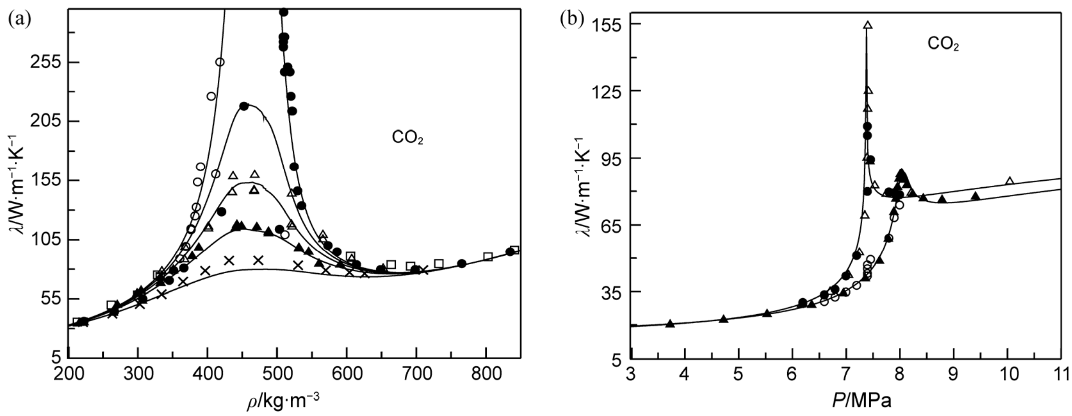

Fig. 10 Measured and calculated thermal conductivities of carbon dioxide along the supercritical isotherms as a function of density (a) and pressure (b). Symbols are reported data from NIST/TRC DATA BASE [125]; Solid curves are calculated from reference correlation by Huber et al. [149] (REFPROP [124]).

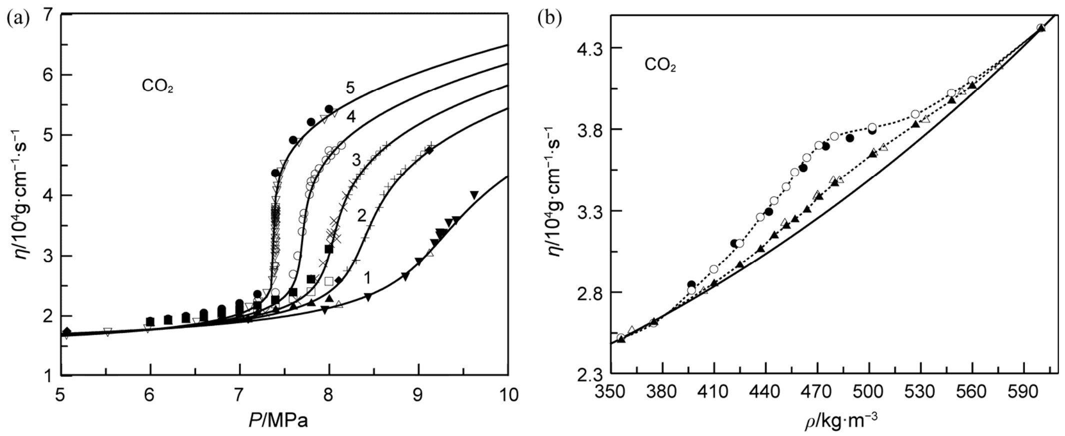

Fig. 11 Measured and calculated viscosities of carbon dioxide along the supercritical isotherms as a function of pressure (a) and density (b). Symbols are reported data from NIST/TRC DATA BASE [125]; Solid curves are calculated from reference correlation by Laesecke and Muzny [150] (REFPROP [124]).

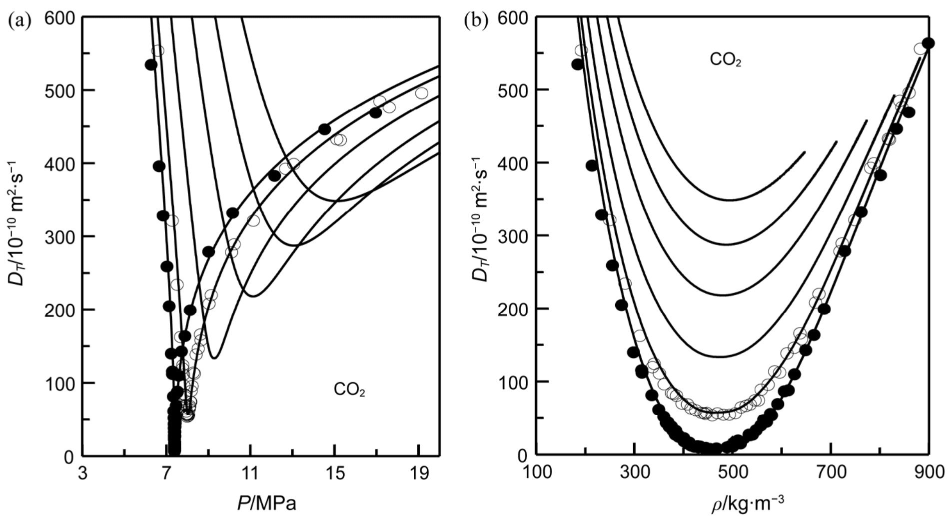

Fig. 12 Measured and calculated thermal diffusivities of carbon dioxide along the supercritical isotherms as a function of pressure (a) and density (b). Symbols are reported data from NIST/TRC DATA BASE [125]; Solid curves are calculated from reference correlation (REFPROP [124]).

subtracts the residual part. As we can note the expression for the fluctuation part of the thermal conductivity depends on the isobaric C_P and isochoric C_V heat capacities, the viscosity η, the correlation length ξ, and a system-dependent cutoff parameter $\overline{q}_D$.

In the asymptotical range of the critical point the isochoric heat capacity, the susceptibility, and correlation length diverge as a simple power laws in the one-phase region ($\Delta\overline{T} \geq 0$) along the critical isochore $\rho = \rho_c$ as [171,172]

$$\overline{C}_V \approx \overline{A}_0 \left(\Delta\overline{T}\right)^{-\alpha}, \quad \overline{\chi} \approx \overline{\Gamma}_0 \left(\Delta\overline{T}\right)^{-\gamma},$$

$$\xi \approx \xi_0 \left(\Delta\overline{T}\right)^{-\nu}, \Delta\overline{\rho}_{\mathrm{cxc}} \approx \pm\overline{B}_0 \left|\Delta\overline{T}\right|^{\beta}. \qquad (8)$$

The critical amplitudes $\overline{A}_0$, $\overline{B}_0$, $\overline{\Gamma}_0$ satisfy a universal relation $\dfrac{\alpha\overline{A}_0\overline{\Gamma}_0}{\overline{B}_0^2} = 0.058 \pm 0.001$. According to the principle of two-scale-factor universality $\xi_0\left(\alpha\overline{A}_0 N_A \rho_c\right)^{1/3} = 0.266 \pm 0.003$. The amplitudes $\overline{A}_0$ and $\overline{B}_0$ are defining from the measured isochoric heat capacity and liquid-gas coexistence curve density data. These amplitudes were used as primary information for developing a correlation

$$\overline{A}_0 = 5.58 + 7.94\omega \quad \text{and} \quad \overline{B}_0 = 1.45 + 1.21\omega \qquad (9)$$

where ω is the acentric factor. The values for $\overline{A}_0$ and $\overline{B}_0$ for some fluids were plotted as a function of the acentric factor ω in Fig. 13. The susceptibility amplitude $\overline{\Gamma}_0$ can then be calculated as $\overline{\Gamma}_0 = \dfrac{0.058\overline{B}_0^2}{\alpha\overline{A}_0}$. Using the derived correlating for the isochoric heat capacity amplitude $\overline{A}_0$, we can estimate the asymptotic critical amplitude for correlation length ξ_0 as $\xi_0 = 0.266\left(\dfrac{v_c}{\alpha\overline{A}_0}\right)^{1/3}$, where $v_c = \left(N\rho_c\right)^{-1}$ is the molecular volume at the critical point. Fig. 14 shows a comparison of the experimental correlation length amplitudes with the values calculated from $\xi_0 = 0.266\left(\dfrac{v_c}{\alpha\overline{A}_0}\right)^{1/3}$. Note that ξ_0 not only depends on $v_c^{1/3}$ but also on the acentric factor ω though $\overline{A}_0$. As one can see, $\xi_0 = 0.266\left(\dfrac{v_c}{\alpha\overline{A}_0}\right)^{1/3}$ provides good prediction for the critical amplitude of correlation length. For represent of the critical fluctuation part of the thermal conductivity, we need to estimate the cutoff parameter $\overline{q}_D$ in Eq. (6). Fig. 14(b) shows the values of $\overline{q}_D^{-1}$ as a function of $v_c^{1/3}$. The values of $\overline{q}_D^{-1}$ are sensitive to the background part of the thermal conductivity λ_b. We value of $\overline{q}_D^{-1}$ correlates with the $v_c^{1/3}$, within the accuracy of cutoff parameter determination. For practical applications, the fluctuation (critical) part of the thermal conductivity $\Delta_c\lambda$ can be expressed by Eq. (6) with the recommended values of universal parameters $R_D = 1.02$, $\overline{T}_R = 1.5$, $\nu = 0.630, \gamma = 1.239$. The crossover model Eq. (6), together with Eq. (7) provides a good representation of the critical anomaly of the thermal conductivity of fluids in the critical and supercritical regions. The practical applications of this equation require an equation of state for the thermodynamic properties and an equation for the viscosity of the fluid. Also, two fluid-dependent asymptotical critical amplitudes ($\overline{A}_0$ and $\overline{B}_0$) and one fluid-specific cutoff wave number $\overline{q}_D$ are required for the thermal conductivity representation. Above described technique can be used when reliable values of the

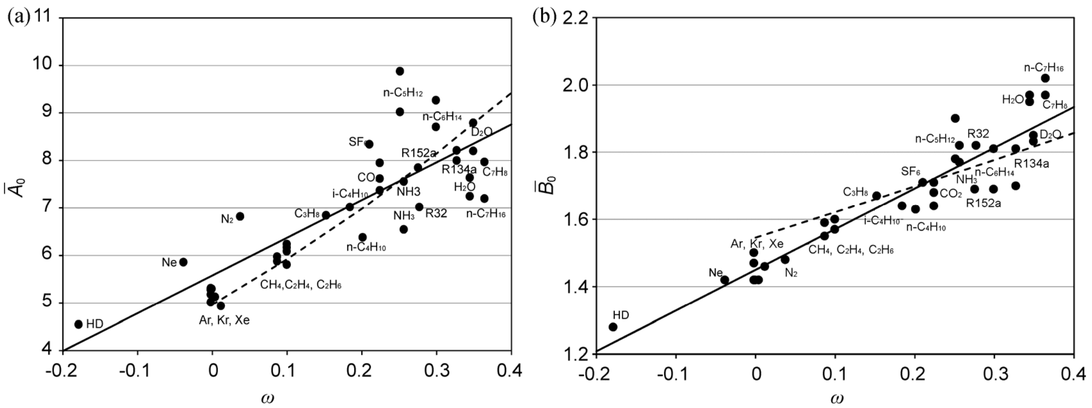

Fig. 13 Heat-capacity ($\overline{A}_0$) and coexistence-curve ($\overline{B}_0$) amplitudes as a function of the acentric factor ω. The symbols are the reported data from the literature (see Ref. [121]). The solid line is calculated from the correlations Eq. (9). The dashed curve is calculated from the correlation equation by Gerasimov [173].

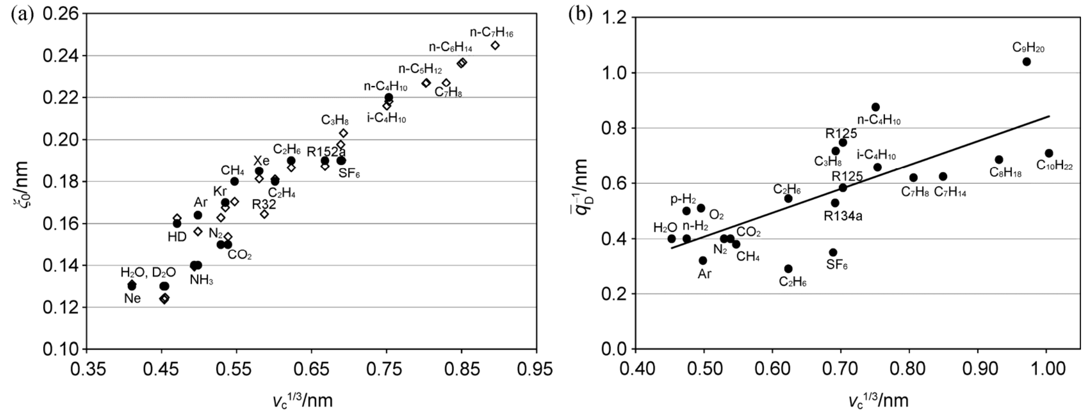

Fig. 14 Correlation-length amplitude ξ_0 (a) and cutoff parameter $\bar{q}_D^{-1}$ (b) as a function of $v_c^{1/3}$. The full circles are the values of reported data from the literature. The open circles are the values of calculated from the correlations Eq. (9).

critical amplitudes ($\bar{A}_0$ and $\bar{B}_0$) are not available. If reliable experimental thermal conductivity data in the critical and supercritical regions are available, then cutoff wave number $\bar{q}_D$ can be determined from a fit to the crossover model. However, for practical calculations it can be well estimated by using the relation $\bar{q}_D^{-1} = -0.0240 + 0.863 v_c^{1/3}$, Therefore, the method described in the present work can be used for quantitative estimates of the fluctuation part of the thermal conductivity of various molecular fluids, even in the case of absence of the reliable experimental thermal conductivity data in the critical and supercritical regions.

3. The Critical Properties of Carbon Dioxide Containing Binary Mixtures and Related Thermodynamic Properties

3.1 The critical properties of binary mixtures CO_2+solute and the Krichevskii parameter

Very limited thermodynamic and transport property data are available for binary CO_2 containing supercritical mixtures (CO_2+solute). In many technological applications (supercritical fluid technology, for example) of supercritical solvents (CO_2), including separations and chemical reactions carried out in such media, the solute is of low volatility (heavy n-alkanes, for example) and is present in small concentrations (dilute mixture, SC solvent+solute). Since isothermal compressibility of pure solvent (CO_2) is diverging at the critical point ($K_T \to \infty$), small changes in the pressure is a result in large changes of the density and, therefore, of the solubility of various low volatility solutes in SC solvent (CO_2). Thermodynamic behavior of infinite dilute mixtures near the critical point depends on microscopic phenomena involving density perturbation induced by the presence of the near- and supercritical solvent and propagation of this density perturbation to a distance given by the solvent's correlation length which $\xi^2 \approx K_T$ (where K_T is the isothermal compressibility of pure solvent, see Fig. 1) [174-179]. The thermodynamic of infinite dilute binary mixtures has wide-ranging scientific interest because of the dominant role played by coexistence of both short- (solvation) and long- (compressibility driven) ranged phenomena [97,174,179] in fluid systems near the critical point of pure solvent. Thermodynamic behavior of the infinite dilute solutions near the critical point of pure solvent is extremely important for understanding of the intermolecular interactions and the microscopic structure of the near- and super-critical solutions where the interaction between solute-solute molecules can be neglected. In the limit of infinite dilution ($x \to 0$), most partial molar properties of the solute such as ($\bar{V}_2^{\infty}, \bar{H}_2^{\infty}, \bar{C}_{P2}^{\infty}$) diverge strongly at the critical point of pure solvent [94,98,180-186]. The thermodynamic properties behavior of infinitely dilute mixtures near the critical point of solvent can be completely determined by the Krichevskii parameter which is equal to the derivative $\left(\frac{\partial P}{\partial x}\right)_{T_C V_C}^{\infty}$ calculated at the critical point of pure solvent (CO_2, for example) [90,94-97,187-191]. Using the concept of the Krichevskii parameter, Levelt-Sengers [191] proposed a description of thermodynamic behavior of dilute near-critical solutions based on the derivative $\left(\frac{\partial P}{\partial x}\right)_{VT}^{\infty}$, or Krichevskii function, $J = \left(\frac{\partial P}{\partial x}\right)_{TV}^{\infty} \left(\frac{\partial^2 A}{\partial V \partial x}\right)^{\infty}$, where A is the Helmholtz free energy. The Krichevskii parameter governs all of the thermodynamic properties of a dilute solution in the vicinity of the critical point of a pure solvent (CO_2). The

Krichevskii parameter plays a crucial role in near-critical solution thermodynamics [191]. For example, the Krichevskii parameter determines the shape of the dew-bubble curves near the critical point, behavior of isotherm in *P-x* space and isobars in *T-x* space, Levelt Sengers [95,97].

The Krichevskii parameter can be readily calculated using initial slopes of the critical lines of binary mixtures using the following relations [97,192,193]

$$\left(\frac{\partial P}{\partial x}\right)^{C}_{V_C T_C} = \left(\frac{\partial P_c}{\partial x}\right)^{C}_{CRL} - \left(\frac{dP_S}{dT}\right)^{C}_{CXC}\left(\frac{\partial T_c}{\partial x}\right)^{C}_{CRL} \quad (10)$$

or, equivalently,

$$\left(\frac{\partial P}{\partial x}\right)^{C}_{V_C T_C} = \left[\left(\frac{dP_c}{dT_c}\right)^{C}_{CRL} - \left(\frac{dP_S}{dT}\right)^{C}_{CXC}\right]\left(\frac{dT_c}{dx}\right)^{C}_{CRL} \quad (11)$$

where $\frac{dT_C}{dx}$ and $\frac{dP_C}{dx}$ are the initial ($x\rightarrow 0$) slopes of the $T_C(x)$ and $P_C(x)$ critical lines, and $\left(\frac{dP_S}{dT}\right)^{C}_{CXC} > 0$ is the slope of the pure solvent's vapor-pressure curve (CO_2) evaluated at the critical point of the solvent (always positive). The regimes near-critical behavior of the dilute mixtures strongly depends on the signs and the magnitudes of the derivatives, $\frac{dT_C}{dx}$, $\frac{dP_C}{dx}$, and $\left(\frac{dP_S}{dT}\right)^{C}_{CXC}$ i.e. on the magnitude and sign of the Krichevskii parameter. Therefore, the direct comparison of the values of the Krichevskii parameter calculated with Eqs. (10) and (11) using the critical properties data and the values estimated from the independent direct measurements of *P-x* dependence along the critical isochore-isotherm of pure solvent (see for example, Abdulagatov et al. [194-197]) provides a good test for the accuracy and consistence of the different type of thermodynamic data. In our previous publications (see Abdulagatov et al. [198,199]), we calculated the value of Krichevskii parameter for the CO_2+solute mixtures with Eqs. (10) and (11) using the measured values of the critical curve data. Measured critical curve data (see our previous publication [201]) for most technologically important CO_2 containing binary mixtures are presented in Figs. 15 to 29. The value of the derivative $\left(\frac{dP_S}{dT}\right)^{C}_{CXC} = 0.1712\ \mathrm{MPa\cdot K^{-1}}$ for pure CO_2 reported by Span and Wagner [200] was used to calculate the Krichevskii parameter together with critical curves data (see our critical lines data compilation [201]). Good agreement was found between the values of the Krichevskii parameter calculated from Eq. (10) using the critical curve properties of the mixture and the values estimated from other thermodynamic data (Henry's constant, distribution coefficient, solubility). Comprehensive review of the critical lines of the CO_2 containing binary mixtures was provided in our earlier publication [201].

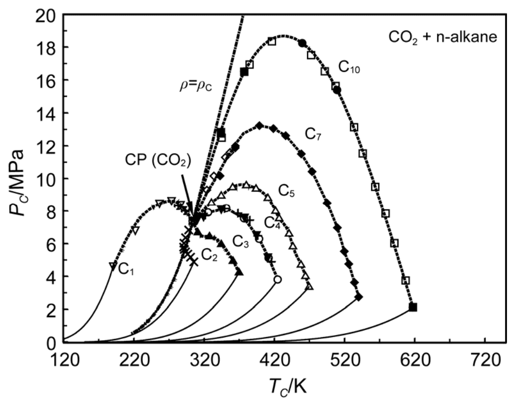

Fig. 15 Reported critical curve data for series of binary CO_2+*n*-alkane mixtures in P_C–T_C projection. Symbols are reported data (see our previous data compilation paper Abdulagatov et al. [201]). Solid lines are vapor-pressure of pure n-alkane calculated from REFPROP, Lemmon et al. [124]. Dotted –dashed line is the critical isochore of pure CO_2.

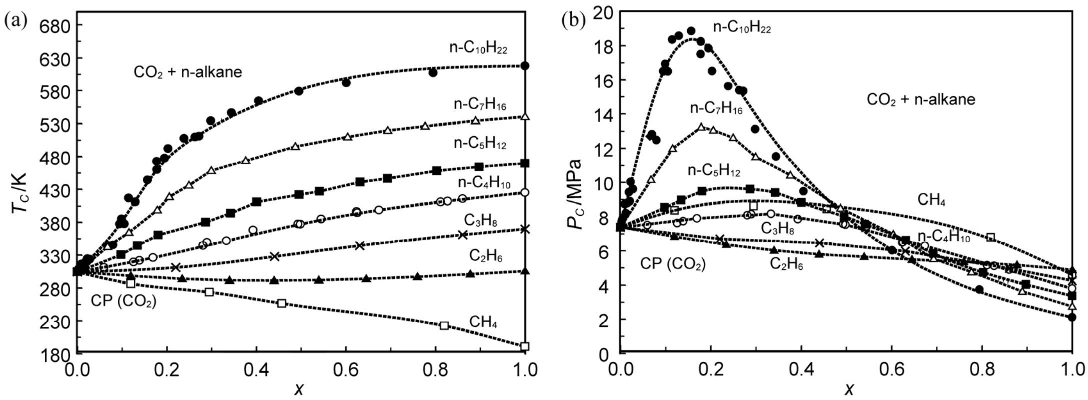

Fig. 16 Reported critical curve data for series of binary CO_2+*n*-alkane mixtures in T_C–*x* (a) and P_C–*x* (b) projections. Symbols are reported data (see our previous data compilation paper Abdulagatov et al. [201]).

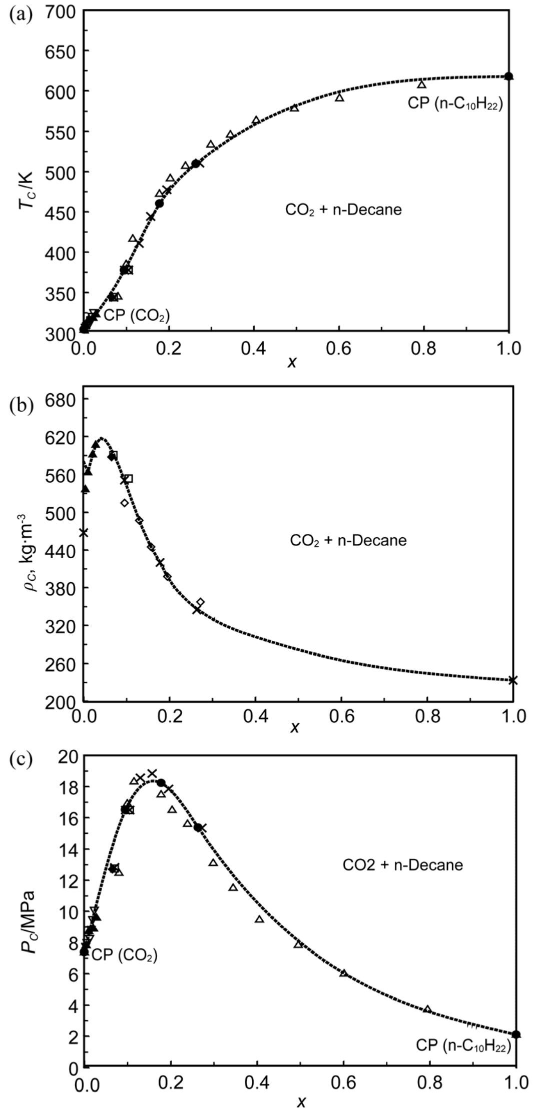

Fig. 17 Reported experimental critical curve data for binary CO_2+*n*-decane mixture in T_C–x, ρ_C–x and P_C–x projections together with our results. ●-Polikhronidi et al. [51-53]. Symbols are reported data (see our previous data compilation paper Abdulagatov et al. [201]).

3.2 Thermodynamic and structural properties of CO_2 containing binary mixtures near the critical point of pure solvent (CO_2)

3.2.1 Thermodynamic properties of dilute mixtures near the critical point of pure solvent and Krichevskii parameter

Long-range density fluctuations, when one of the component of the mixture (solvent, CO_2) in the critical region, the mixture exhibit critical enhancement of the thermodynamic and transport properties (critical anomaly) [93-97]. For example, solute partial molar properties ($\overline{V}_2^\infty, \overline{H}_2^\infty, \overline{C}_{P2}^\infty$) in the immediate vicinity of the solvent's (CO_2) critical point are diverging. Partial molar properties ($\overline{V}_2^\infty, \overline{H}_2^\infty, \overline{C}_{P2}^\infty$) are directly related with the Krichevskii parameter and critical curves behavior (see for example, Abdulagatov et al. [198,199]). The partial molar volume at infinite dilution, $\overline{V}_2^\infty$, is a very fundamental solution property [93-98]. It can be expressed as a simple integral by using the direct correlation function (DCF) [174-176] (see below). The partial molar volumes, $\overline{V}_2^\infty$, of hydrocarbons in CO_2 interest for calculation solubility using Henry's law, especially near the critical point of pure CO_2 where $\overline{V}_2^\infty$ increases strongly with increasing compressibility K_T of pure CO_2 and diverges at the critical point of the pure solvent. The partial molar volume $\overline{V}_2^\infty$ can be calculated using the Krichevskii function as $\left(\frac{\partial P}{\partial x}\right)_{TV}^\infty$ [95,174-176]

$$\overline{V}_2^\infty = \rho^{-1}\left[K_T\left(\frac{\partial P}{\partial x}\right)_{TV}^\infty + 1\right] \tag{12}$$

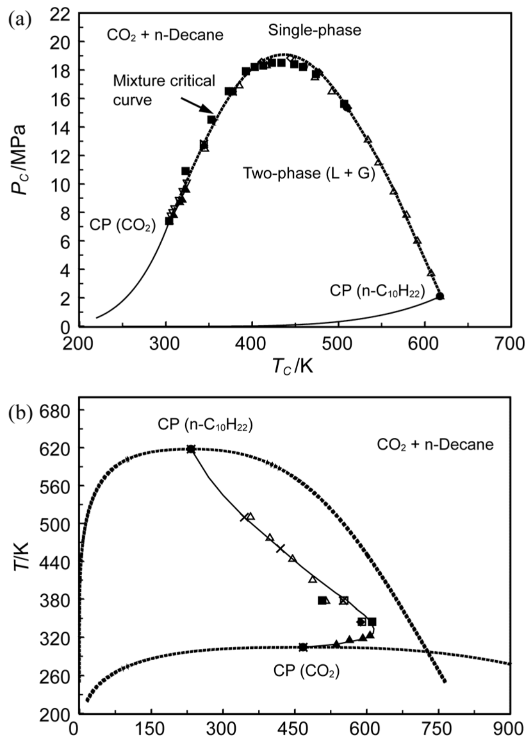

Fig. 18 Reported experimental critical curve data for binary CO_2+*n*-decane mixture together with our results in P_C–T_C and ρ_C–T_C projections. ●-Polikhronidi et al. [51-53]. Symbols are reported data (see critical curve data compilation [201]). Solid lines are pure component vapor – pressure curves calculated from reference EOS (REFPROP, Lemmon et al. [124]).

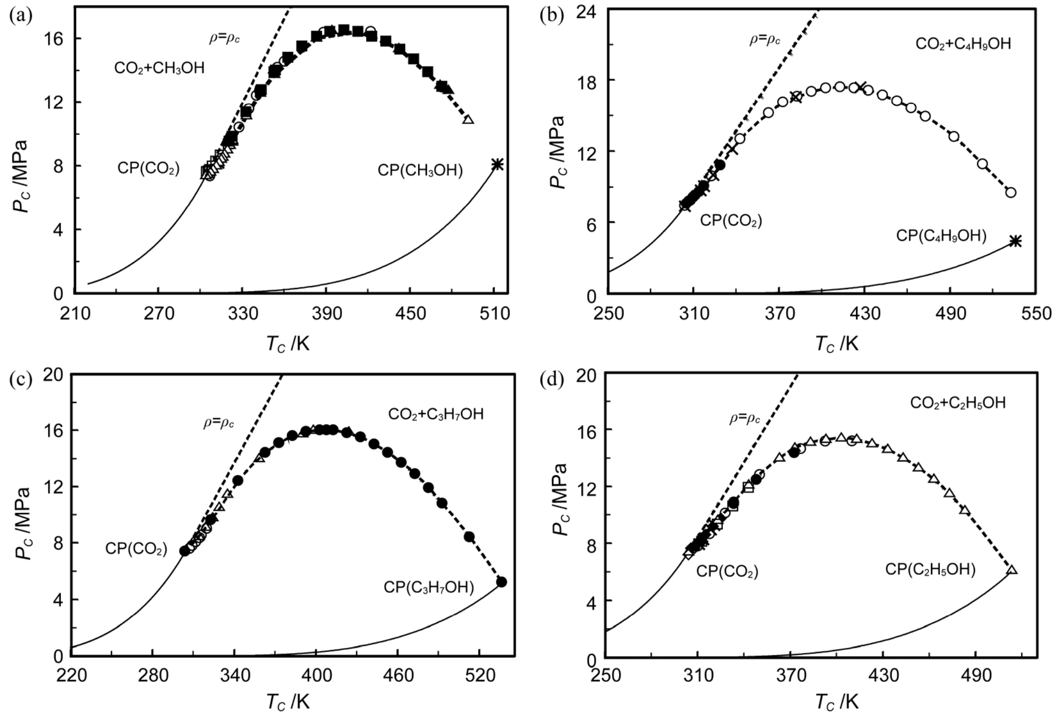

Fig. 19 P_C–T_C projection of the critical lines of CO_2+solute (alcohols) reported by various authors together with vapor-pressure curve for pure components. Symbols are reported data (see critical curve data compilation [201]).

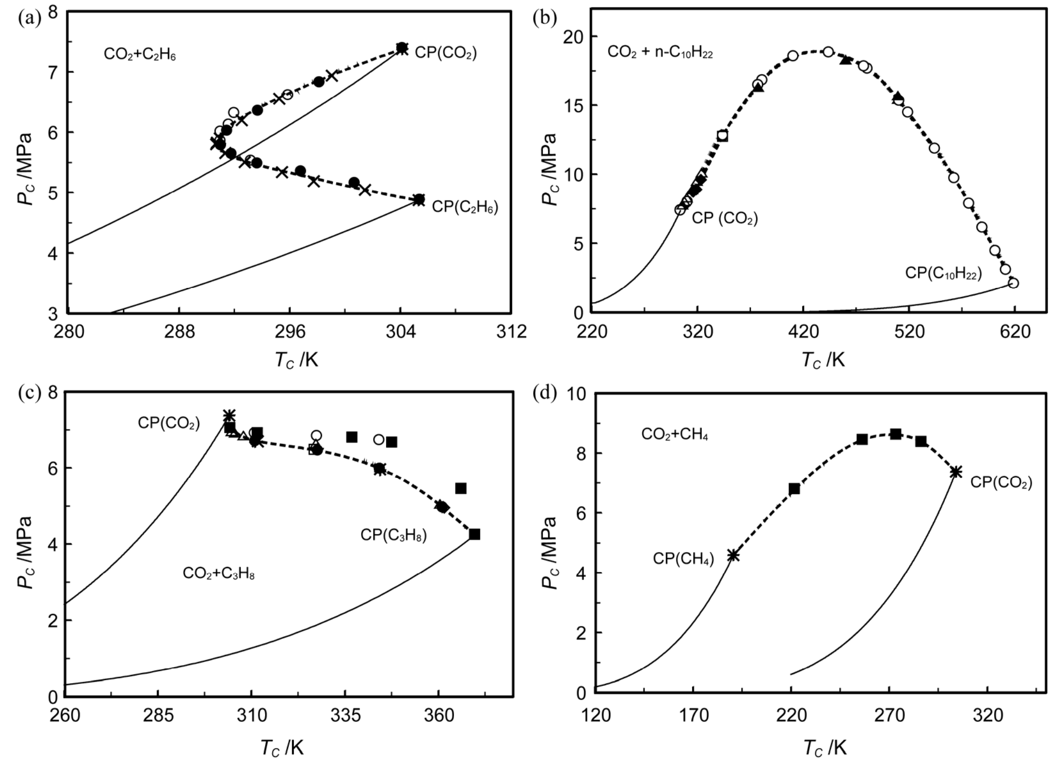

Fig. 20 P_C–T_C projections of the critical lines of CO_2+C_2H_6, CO_2+n-$C_{10}H_{22}$, CO_2+n-C_3H_8 and CO_2+CH_4 mixtures reported by various authors. Symbols are reported data (see critical curve data compilation [201]). Dashed lines are from crossover model [102,153-157]; Solid curves are vapor-pressure curves of the pure components (REFPROP [124]).

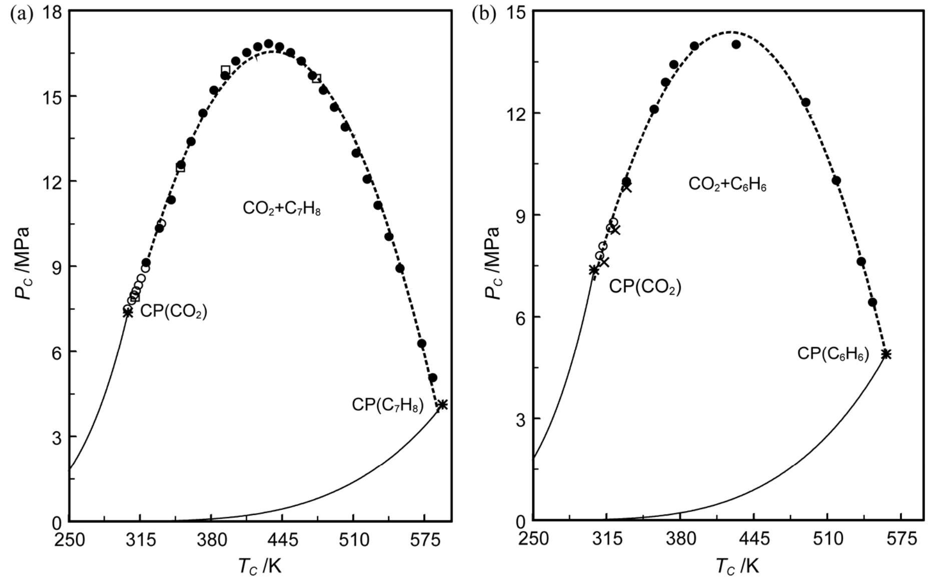

Fig. 21 P_C–T_C critical curves behavior of $CO_2+C_7H_8$ and $CO_2+C_6H_6$ mixtures reported by various authors. Solid curves are vapor-pressure curves of pure components calculated from REFPROP [124]. Symbols are reported data (see critical curve data compilation [201]).

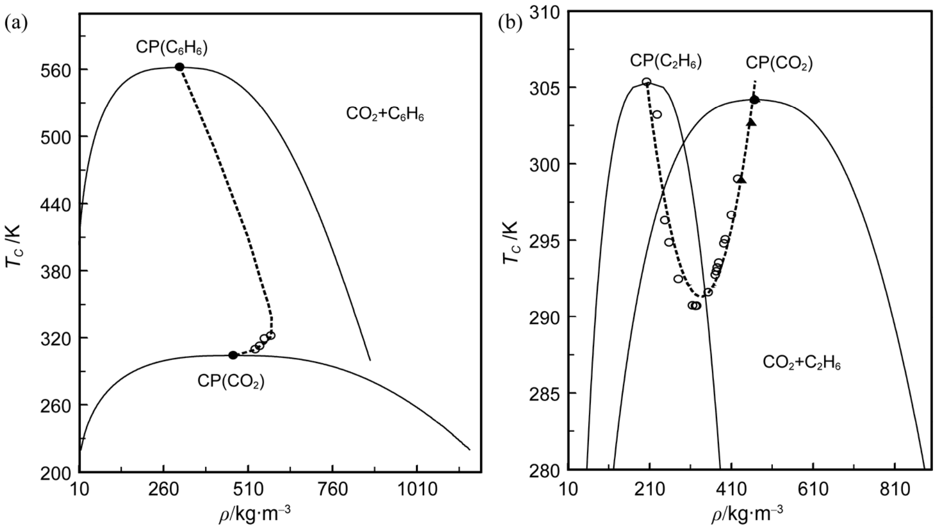

Fig. 22 Behavior of the T_C–ρ_C projection of the critical curve of $CO_2+C_6H_6$ and $CO_2+C_2H_6$ mixtures reported by various authors. Solid curves are liquid+gas coexistence curves of pure components calculated from REFPROP [124]. Symbols are reported data (see critical curve data compilation [201]).

where K_T and ρ are the compressibility and density of pure solvent, respectively. In the vicinity of the solvent's critical point, $T \to T_C$, isothermal compressibility diverges as $K_T \propto \left(T - T_C\right)^{-\gamma} \to +\infty$, therefore, the partial molar volume $\overline{V}_2^\infty$ also diverges strongly like K_T. The Krichevskii function J does not diverge at the solvent's critical point and can be used to describe the behavior of dilute binary systems. The sign of the partial molar volume $\overline{V}_2^\infty$ depends on the sign of the Krichevskii parameter because K_T>0 is always positive and values of the $K_T\left(\frac{\partial P}{\partial x}\right)_{TV}^\infty >> 1$ near the critical point. Depending on the chemical nature of the solute molecules, the values of partial molar volume tends to $\overline{V}_2^\infty \to +\infty$ or $\overline{V}_2^\infty \to -\infty$ (see Figs. 30 to 32). This anomaly is caused by the critical effects due to the divergence of the isothermal compressibility K_T of the pure solvent and is common for all dilute near-critical mixtures [93-95,97]. According to the scaling theory, $\overline{V}_2^\infty$ diverges along the solvent's critical isotherm-isochore as ($x^{-1+\gamma/\beta\delta}$) [93-95,97,202-204].

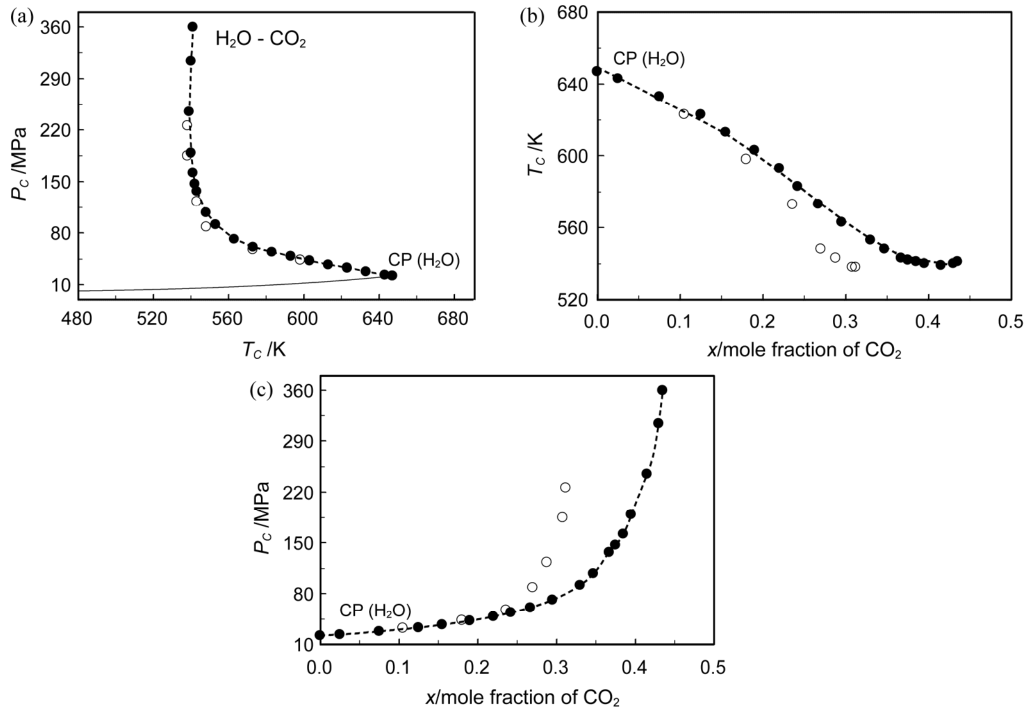

Fig. 23 P_C–T_C, T_C–x and P_C–x critical curves for CO_2+H_2O mixture reported by various authors. Symbols are reported data (see critical curve data compilation [201]).

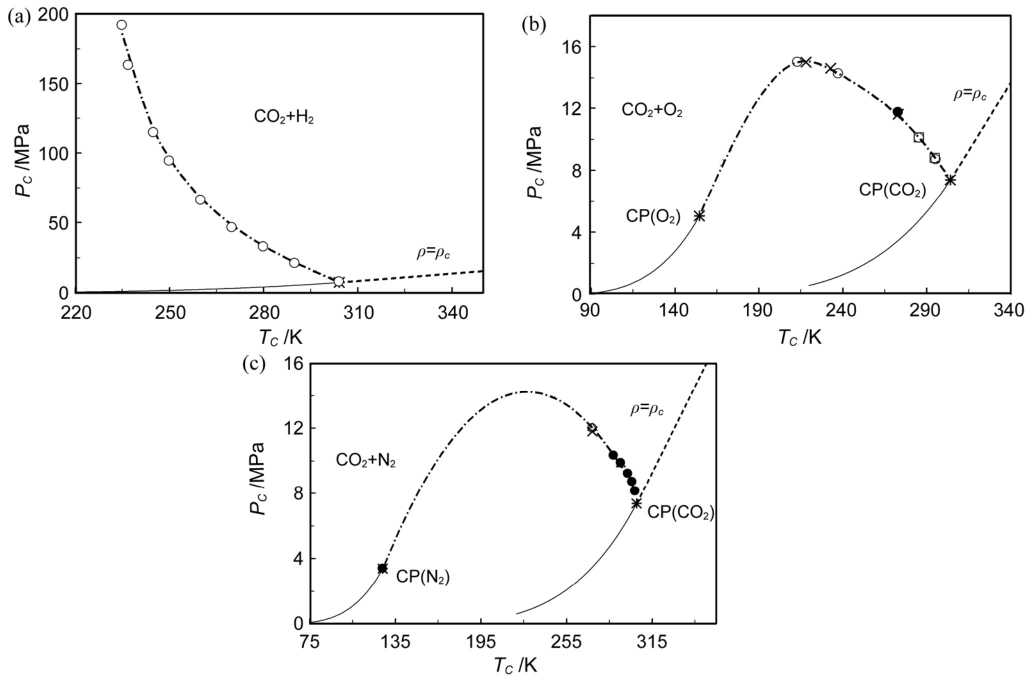

Fig. 24 P_C–T_C projections of the critical lines of binary carbon dioxide containing mixtures CO_2+H_2, CO_2+O_2, and CO_2+N_2 reported by various authors Symbols are reported data (see critical curve data compilation [201]). Solid curves are vapor-pressure curves for pure components [124]. Dashed-dotted curve is the critical isochore of pure CO_2.

For the classic theory (γ=1, β=0.5, δ=3), $\bar{V}_2^{\infty} \propto x^{-1/3}$ and for the non-classical case (γ=1.24, β=0.325, δ=4.83), $\bar{V}_2^{\infty} \propto x^{-0.2133}$. Adding a solute molecules to the critical solvent (CO_2) which will likely raise the pressure, $\left(\dfrac{\partial P}{\partial x}\right)_{\mathrm{TV}}^{\mathrm{C}} > 0$ (Krichevskii function is positive), will

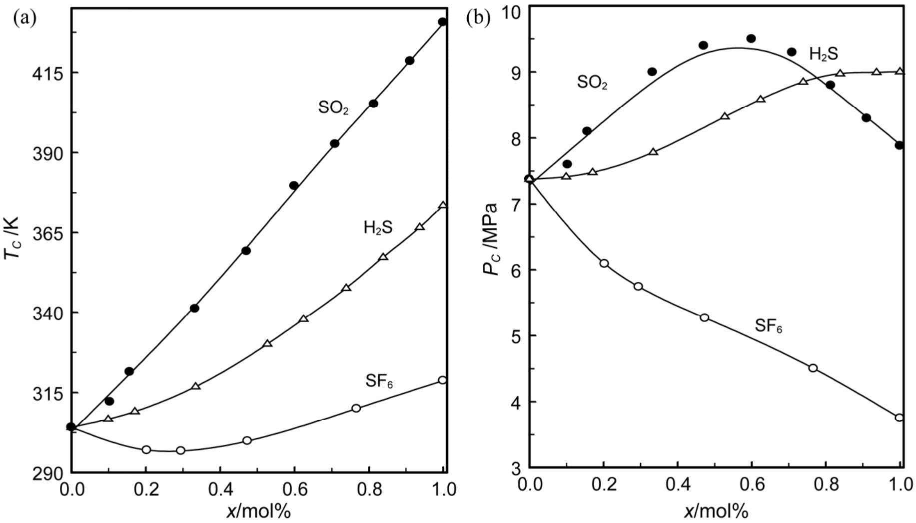

Fig. 25 T_C–x and P_C–x projections of the critical lines of binary carbon dioxide containing mixtures CO_2+SO_2, CO_2+H_2S , and CO_2+SF_6 reported by various authors. Symbols are reported data (see critical curve data compilation [201]).

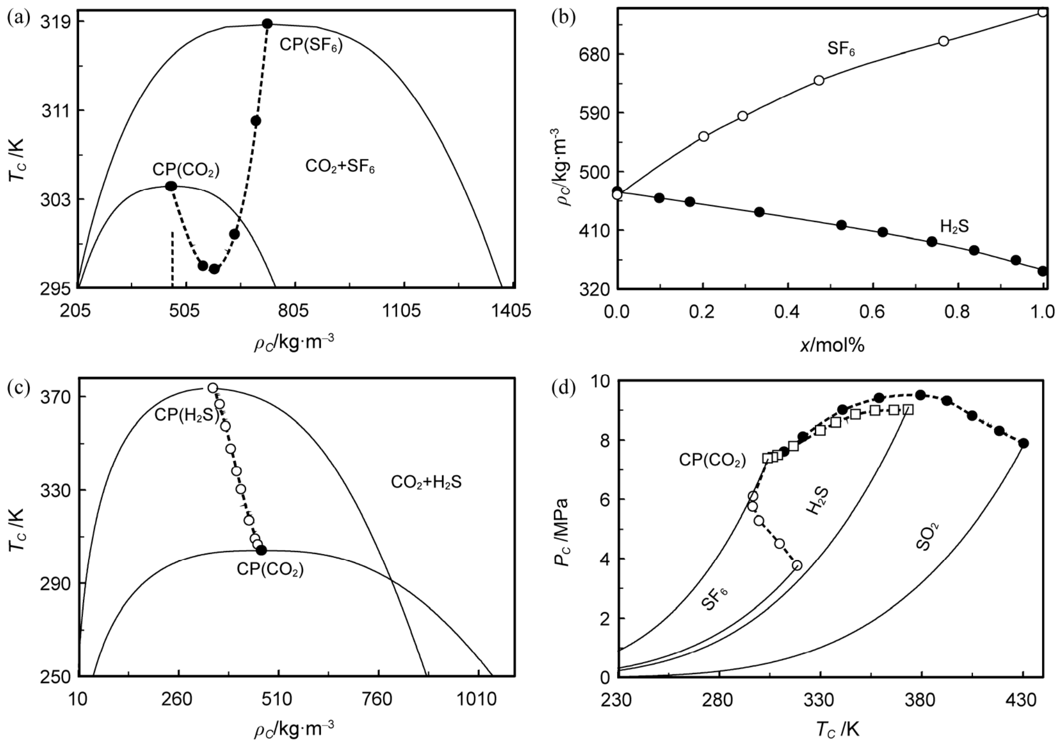

Fig. 26 T_C–ρ_C, ρ_C–x and P_C–T_C projections of the critical lines of binary carbon dioxide containing mixtures CO_2+SF_6, CO_2+H_2S and CO_2+SO_2 reported by various authors. Symbols are reported data (see critical curve data compilation [201]). Solid curves are vapor-pressure curves for pure components [124].

cause the positive divergence of the partial molar volume $\bar{V}_2^{\infty} \to +\infty$. For binary mixtures of CO_2+n-alkane (n>5), CO_2+alcohol and CO_2+acetone, the negative divergence of the $\bar{V}_2^{\infty} \to -\infty$ was observed (see Figs. 30 to 32), therefore, the negative divergence of the derivative $\left(\frac{\partial V_m}{\partial x}\right)_{PT}^{\infty} \to -\infty$, and the Krichevskii parameters for these systems are negative, $\left(\frac{\partial P}{\partial x}\right)_{\mathrm{TV}}^{\mathrm{C}} < 0$. However, for low n-alkanes (n<5, see Fig. 33) and noble gases (Ne, Kr, for example) the values of the Krichevskii parameter are positive, therefore, partial molar volumes for these mixtures are positively diverging. Also, the derivative, $\left(\frac{\partial H_m}{\partial x}\right)_{PT} \approx T\alpha_P \left(\frac{\partial P}{\partial x}\right)_{TV}^{C}$, therefore, the partial molar enthalpy $\bar{H}_2^{\infty}$ of the solute diverges as the isobaric expansion coefficient α_P of pure solvent, which in turn diverges as the isothermal compressibility K_T. The partial molar heat capacity $\bar{C}_{P2}^{\infty}$ related with the partial molar enthalpy as $\bar{C}_{P2}^{\infty} = \left(\partial \bar{H}_2^{\infty} / \partial T\right)_P$, therefore, the values of $\bar{C}_{P2}^{\infty}$ already diverge at the critical point of pure CO_2, but its divergence is much stronger than that of the partial molar volume and enthalpy.

The Krichevskii parameter, derived from the critical curves data, plays the crucial role in the study of other properties of near-critical dilute solutions such as Henry's

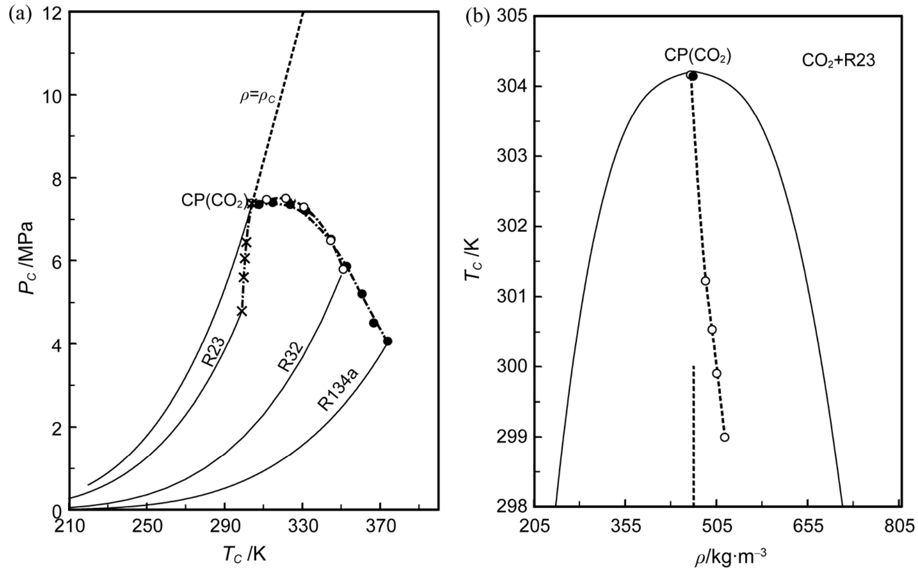

Fig. 27 P_C–T_C and T_C–ρ_C projections of the critical lines of binary carbon dioxide containing mixtures CO_2+R23, CO_2+R32, and CO_2+R134a reported by various authors. Symbols are reported data (see critical curve data compilation [201]). Solid curves are vapor-pressure and liquid+gas coexistence curves for pure components [124].

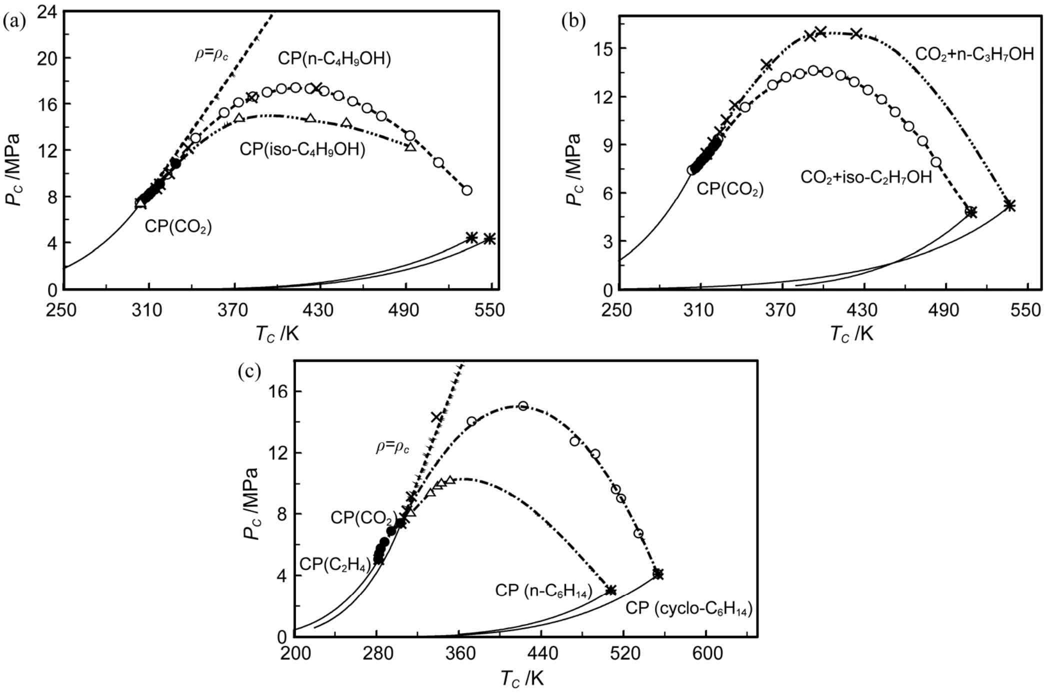

Fig. 28 P_C–T_C projections of the critical lines of binary carbon dioxide containing mixtures CO_2+n-C_4H_9OH, CO_2+n-C_3H_7OH, and CO_2+n-C_6H_{12} reported by various authors. Symbols are reported data (see critical curve data compilation [201]). Solid curves are vapor-pressure curves for pure components [124].

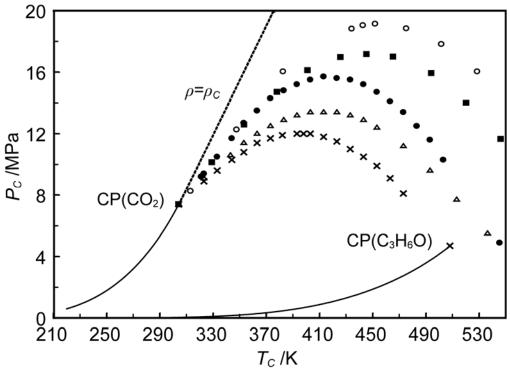

Fig. 29 P_C–T_C projection of the critical line for CO_2+solute (some complex organic compounds) reported by various authors. Symbols are reported data (see critical curve data compilation [201]). Solid curves are vapor-pressure curves for pure components [124]. ●- acetonitryl; ○-pyridine; Δ-chloroform; ■-acetic acid; ×- acetone.

constant, K_H, distribution equilibrium constant, and the solubility [188,205-208]. The value of the Krichevskii parameter can be calculated from the Henry's constant K_H [187,188] near the critical point as

$$T\ln\left[\frac{K_H}{f_1}\right]=A+B\left(\rho-\rho_C\right) \tag{12}$$

or

$$T\ln E=A+B\left(\rho-\rho_C\right) \tag{13}$$

where K_H is the Henry's constant defined as $K_H=\lim_{x_2\to 0}\left(f_2/X_2\right)$ and f_2 is the fugacity of a solute, f_1 is the fugacity of the pure solvent; ρ is the liquid phase density of the pure solvent along the liquid-gas coexistence curve, and ρ_C is the solvent's critical density; $E=y_2P/P_2^{sub}$ is the enhancement factor, and P, y_2, P_2^{sub} are the pressure, solubility, and sublimation pressure, respectively. The values of constant B is related to the Krichevskii parameter by

$$\left(\frac{\partial P}{\partial x}\right)_{T_CV_C}^{\infty}=R\rho_C^2B \tag{14}$$

Near the critical point, (ρ–ρ_C) approaches to zero as $(T–T_C)^{\beta}$, therefore the temperature derivative of Henry's constant diverges as $(T–T_C)^{\beta-1}$. Eqs. (12) and (13) imply that $T\ln\left[\frac{K_H}{f_1}\right]$ and $T\ln E$ are linear in the solvent density, with a slope given by the Krichevskii parameter.

The Krichevskii parameter can be also calculated from vapor-liquid distribution factor [187,191,208,209] K_D which is defined as $K_D=\lim_{x_2,y_2\to 0}\left(Y_2/X_2\right)_T$, where Y_2 and X_2 are the molar functions of the solute in the vapor and liquid phase, respectively. At the critical conditions the vapor-liquid distribution factor K_D related to the Krichevskii parameter by [206,209]

$$T\ln K_D=2\left[\frac{\partial P}{\partial x}\right]_{T_CV_C}^{\infty}\frac{1}{R\rho_C^2}\left(\rho-\rho_C\right) \tag{15}$$

As one can see from this relation, the value of Krichevskii parameter can be estimated from the slope of the plot $T\ln K_D$ versus (ρ–ρ_C) or $T\ln\left[\frac{K_H}{f_1}\right]$ versus

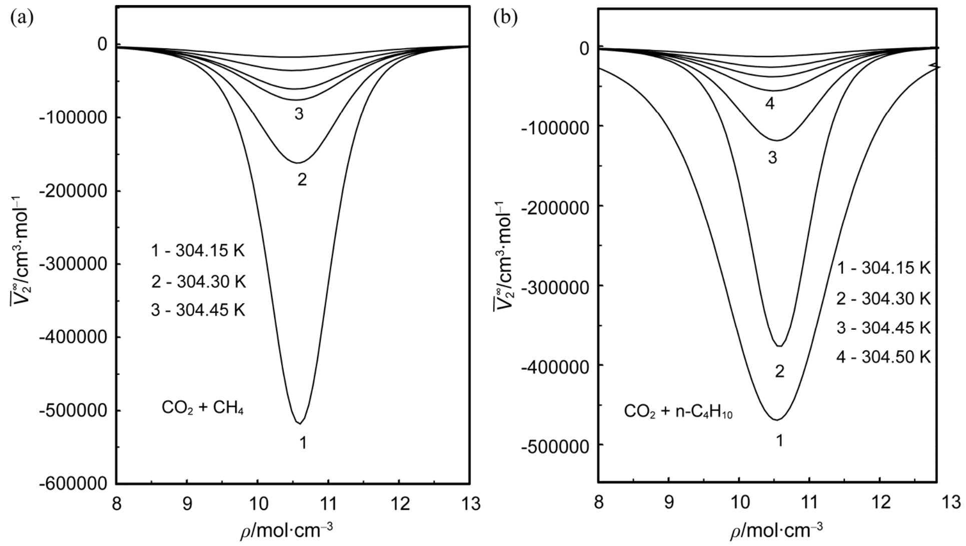

Fig. 30 Partial molar volumes $\overline{V}_2^{\infty}$ of CO_2 containing binary mixtures CO_2+CH_4 and CO_2+n-C_4H_{10} along the supercritical isotherms of pure CO_2 calculated from Eq. (12) and crossover model [102,153-157].

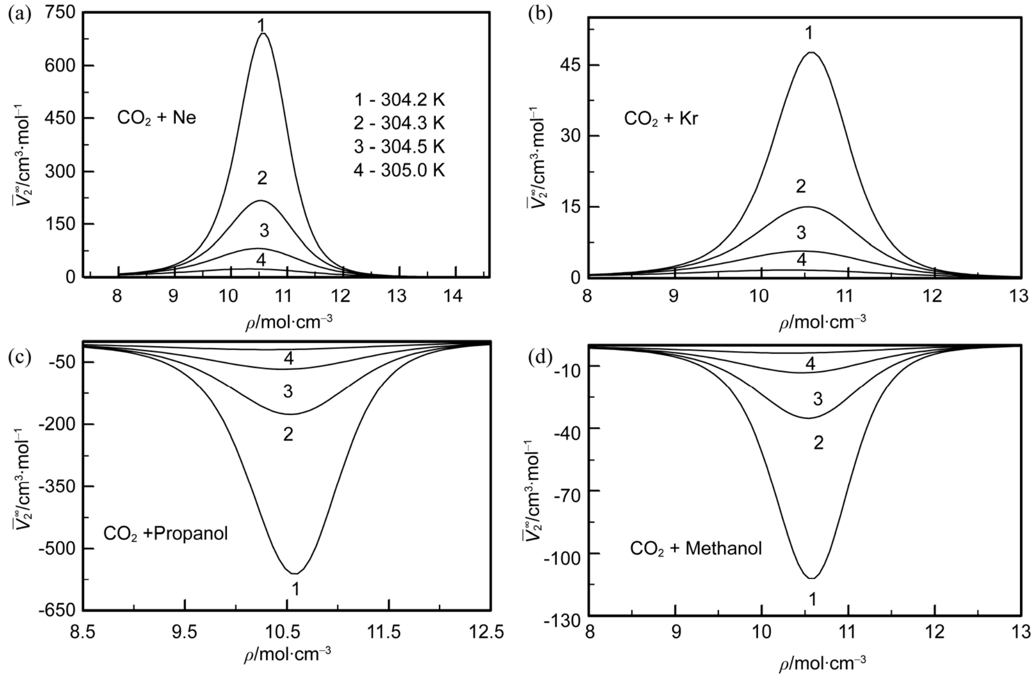

Fig. 31 Partial molar volumes $\bar{V}_2^{\infty}$ of CO_2 containing binary mixtures CO_2+Ne, CO_2+Kr, CO_2+C_3H_7OH and CO_2+CH_3OH along the supercritical isotherms of pure CO_2 calculated from Eq. (12) and crossover model [102,153-157].

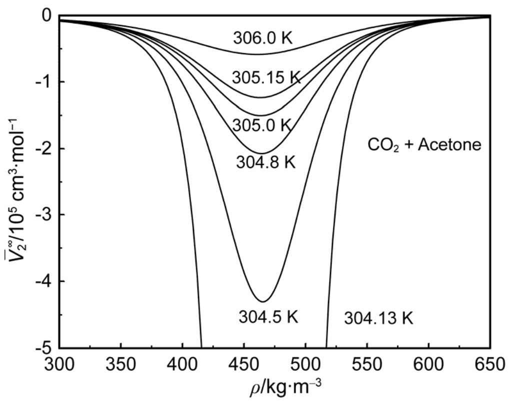

Fig. 32 Partial molar volumes $\bar{V}_2^{\infty}$ of CO_2 containing binary mixture CO_2+aceton along the supercritical isotherms of pure CO_2 calculated from Eq. (12) and crossover model [102,153-157].

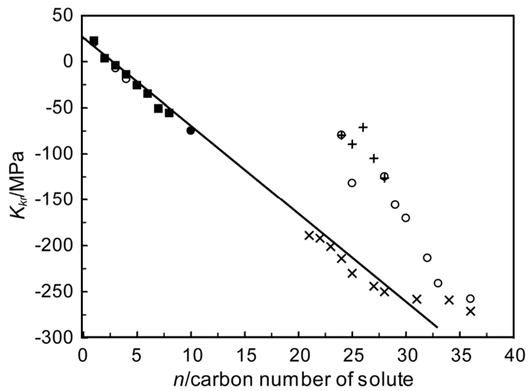

Fig. 33 Krichevskii parameter of binary systems of CO_2 +n-alkane as a function of carbon number of solute (n-alkane) reported by various authors. ●- $C_{10}H_{22}$ (Polikhronidi et al. [51-53]); ○-Furuya and Teja [190]; Δ-chloroform; ■-Abdulagatov et al. [201]; ×-Roth [211]; and + - Furuya and Teja [212].

$(\rho-\rho_C)$. The linearity of $T\ln K_D$ versus $(\rho-\rho_C)$ or $T\ln\left[\frac{K_H}{f_1}\right]$ versus $(\rho-\rho_C)$ curves is strongly supported by experiments. Mendez-Santiago and Teja [210] have compiled available solid-supercritical fluid data and showed that Eq. (13) is valid over a wide range of temperatures and pressures, including solvent reduced pressures up to 2.5. In this work [210] the solubility data were correlated using Eq. (12), and best-fit values of the slope A and intercept B (Krichevskii parameter) were determined. Japas et al. [209] reported the Krichevskii functions and parameters for some mixtures from solubility of the solids in a variety of near-critical solvents.

The distribution constant K_D correlation equation was developed by Plyasunov and Shock [207]. This equation given by

$$\ln K_D = n\ln\left(\frac{\rho(l)}{\rho(V)}\right) + V^3\left(F + Gv + Hv^2\right) \qquad (16)$$

where coefficient n related to the Krichevskii parameter by means of

$$n = \left(\frac{\partial P}{\partial x}\right)^{\infty}_{iT_C V_C} \frac{V^0_{1,C}}{RT_C} \approx \frac{1}{96.17}\left(\frac{\partial P}{\partial x}\right)^{\infty}_{iT_C V_C} \quad (17)$$

Harvey [189] showed that $RT\ln x$, where x the mole fraction of the solute in the supercritical phase in the presence of inert pure solid as a second phase, is linear in the solvent density, with the Krichevskii parameter, divided by ρ_C^2

$$RT\ln x = C_1 - (\rho - \rho_C)\frac{\left(\frac{\partial P}{\partial x}\right)^{\infty}_{T_C V_C}}{\rho_C^2} + \Lambda \quad (18)$$

where C_1 is the constant. Therefore, the comparison of the Krichevskii parameter derived with critical curves data from Eqs. (10) and (11) and from other independent measurements of the Henry's constant, distribution coefficient, and solubility are a good test for the thermodynamic consistence among various type measurements.

3.2.2 Structural properties of the supercritical CO_2 containing binary mixtures

The structural (direct, C_{ij}, and total, H_{ij}, correlation integrals and cluster's size, N^{∞}_{exc}) properties of infinite dilution mixtures are also directly related with the Krichevskii parameter and critical curves behaviour. Thermodynamic behaviour of dilute mixtures is extremely important for the understanding of solute and solvent molecular interactions and the microscopic structure of solutions near the critical point of pure solvent (CO_2). The Krichevskii function is related with the total correlation function integral (TCFI) as [213]

$$\left(\frac{\partial P}{\partial x}\right)^{\infty}_{TV} = \frac{\rho(H_{11} - H_{12})}{K_T} \quad (19)$$

where H_{11} and H_{12} are the TCFI defined as $H_{ij} = \int h_{ij}(r)dr$; $h_{ij}(r) = g_{ij}(r) - 1$ is the total correlation function for i-j pair interactions; $g_{ij}(r)$ is the radial distribution function; and $H_{11} = (K_T RT) - \rho^{-1}$ is the TCFI for i-i pair (pure solvent CO_2 molecules) interactions; K_T and ρ are the isothermal compressibility and density of pure solvent (CO_2), respectively. In terms of the direct correlation function, $c_{ij}(r)$, for i-j pair interactions, the Krichevskii function J is defined as [186,213,214]

$$J = RT\rho^2 (C_{11} - C_{12}) \quad (20)$$

where C_{11} and C_{12} are the direct correlation function integrals (DCFI) defined as $C_{ij} = \int c_{ij}(r)\mathrm{d}r$; and $(1 - \rho C_{11}) = (\rho K_T RT)^{-1}$ is the DCFI for i-i (pure solvent CO_2 molecules) pair interactions. The DCFI's are related to the TCFI by the integrated Ornstein-Zernike equation [165] as

$$H_{12} = C_{12} + \rho C_{12} H_{11} \quad (21)$$

The DCFI (C_{12}) and TCFI (H_{12}) are also can be expressed by partial molar volume at infinity dilution as [214,215]

$$-C_{12} = \frac{\bar{V}_2^{\infty}}{K_T RT_{\rho}} - V \text{ and } \bar{V}_2^{\infty} = V + (H_{11} - H_{12}) \quad (22)$$

The values of direct (C_{12}) and (C_{11}) correlation function integrals for binary carbon dioxide containing mixture CO_2+n-butane are depicted in Fig. 34 . Eq. (22) can be used to calculate the DCFI and TCFI from the partial molar volumes $\bar{V}_2^{\infty}$, therefore, to calculate the microscopic intermolecular potential function parameters using the relation between the direct and total correlation functions and interaction potential function $u_{ij}(r)$ (Percus-Yevick approximation). The value of the

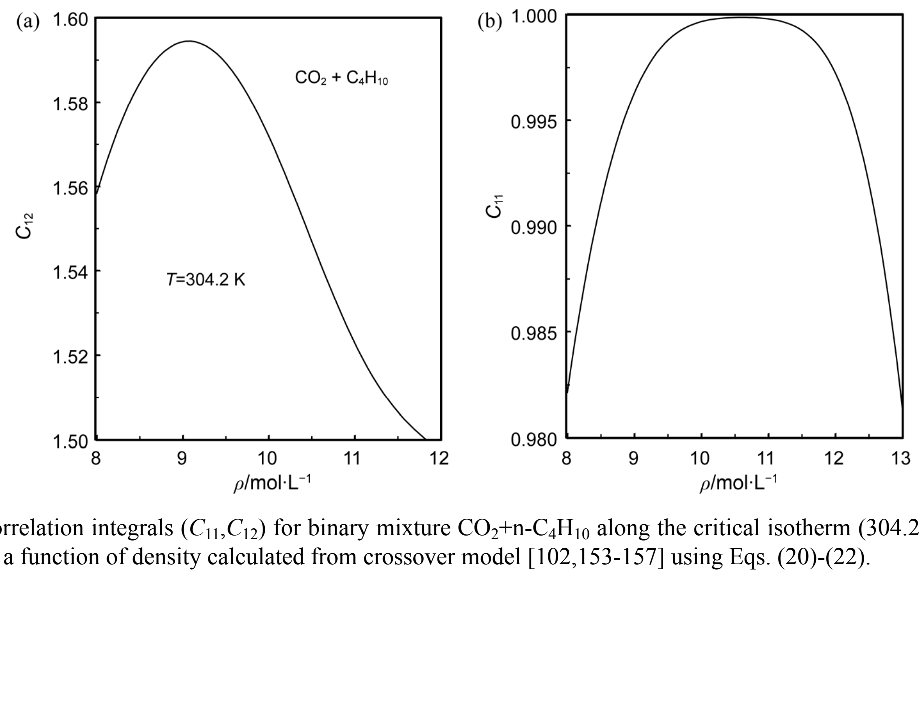

Fig. 34 Direct correlation integrals (C_{11},C_{12}) for binary mixture CO_2+n-C_4H_{10} along the critical isotherm (304.2 K) of pure solvent (CO_2) as a function of density calculated from crossover model [102,153-157] using Eqs. (20)-(22).

Krichevskii function, J, also associated with the behavior of the microstructure of the dilute mixture (see below), measures the finite microscopic rearrangement of the solvent structure around the infinitely dilute solute relative to the solvent structure of ideal solution. The Krichevskii function is defining the structural properties of infinite dilute mixtures, namely, the excess number of solvent molecules $N^{\infty}_{\mathrm{exc}}$ (structural parameter) around the infinitely dilute solute relative to that number around any other solvent molecule as [214]

$$N^{\infty}_{exc} = -K_T \left(\frac{\partial P}{\partial x}\right)^{\infty}_{\mathrm{TV}} \tag{23}$$

where $N^{\infty}_{exc} = 4\pi\rho \int_0^{R_{shell}} \left[g_{12}(r) - g_{11}(r)\right] r^2 dr$, is the definition of the excess number of solvent molecules surrounding molecule of the solute. As one can see from this relation, $N^{\infty}_{\mathrm{exc}} = N_{12} - N_{11}$, where $N_{12} = 4\pi\rho \int_0^{R_{shell}} g_{12}(r) r^2 dr$ and $N_{11} = 4\pi\rho \int_0^{R_{shell}} g_{11}(r) r^2 dr$ are the coordination numbers for the first solvation shell (molecule clusters). N_{12} is indicating the number of solute molecules surrounded by a cage of N_{12} molecules of solvent, while N_{11} indicating that each solvent molecule in the bulk surrounded by a cage of N_{11} other solvent molecules. Since isothermal compressibility goes to infinity at the solvent critical point, $K_T \to +\infty$, therefore, the cluster size also goes to infinity $N^{\infty}_{exc} \to \pm\infty$ depending on the Krichevskii parameter sign. The discontinuity of $N^{\infty}_{\mathrm{exc}}$ is the result of long range (critical) part of the radial distribution function $g_{ij}(r)$. As one can see from Fig. 35, for CO_2+acetone and CO_2+n-butane mixtures, the values of $N^{\infty}_{\mathrm{exc}}$ are positively infinite at the critical point of pure CO_2.

4. Isochoric Heat Capacity Maxima-Minima Loci for Supercritical CO_2

Fig. 5 shows the density dependence of the measured one-phase C_{V} along the selected supercritical isotherms for CO_2 together with the values calculated from reference fundamental (Span and Wagner [123], REFPROP [124]) and crossover (KIselev et al. [153-157]) equation of state. One- phase isochoric heat capacities are also providing valuable theoretical information on temperature derivatives $\left(\partial^2 P/\partial T^2\right)_{\rho}$ of P-T isochores behavior of fluids in the supercritical region and at densities of $\approx 2\rho_{\mathrm{C}}$. For example, it is well-known [216-226] that one-phase C_{V}–ρ dependence provides very useful information about qualitative behavior of P–T isochores curvature, $\left(\partial^2 P/\partial T^2\right)_{\rho}$, i.e., qualitative behavior of the thermodynamic PVT surface (phase-diagram) in the critical and supercritical regions. Second temperature derivatives of pressure, $\left(\partial^2 P/\partial T^2\right)_{\rho}$ and vapor-pressure, $\left(\mathrm{d}^2 P_{\mathrm{S}}/\mathrm{d}T^2\right)$, for carbon dioxide can be directly calculated from the measured values of C_{V} in the one-phase region as a first density derivative, $\left(\partial C_{\mathrm{V}}/\partial\rho\right)_{\mathrm{T}}$ and two-phase liquid $\left(C'_{\mathrm{V2}}\right)$ and vapor C''_{V2} measurements at saturation as [54,55,130-132]

$$\left(\frac{\partial^2 P}{\partial T^2}\right)_{\rho} = -\frac{\rho^2}{T}\left(\frac{\partial C_V}{\partial \rho}\right)_{\mathrm{T}} \tag{24}$$

$$\frac{\mathrm{d}^2 P_{\mathrm{S}}}{\mathrm{d}T^2} = \frac{C''_{\mathrm{V2}} - C'_{\mathrm{V2}}}{T\left(V'' - V'\right)} \tag{25}$$

Thus, one- and two-phase C_{V} measurements as a function of specific volume (or density) are defining the real curvature, $\left(\partial^2 P/\partial T^2\right)_{\rho}$ and $\left(\mathrm{d}^2 P_{\mathrm{S}}/\mathrm{d}T^2\right)$, of the

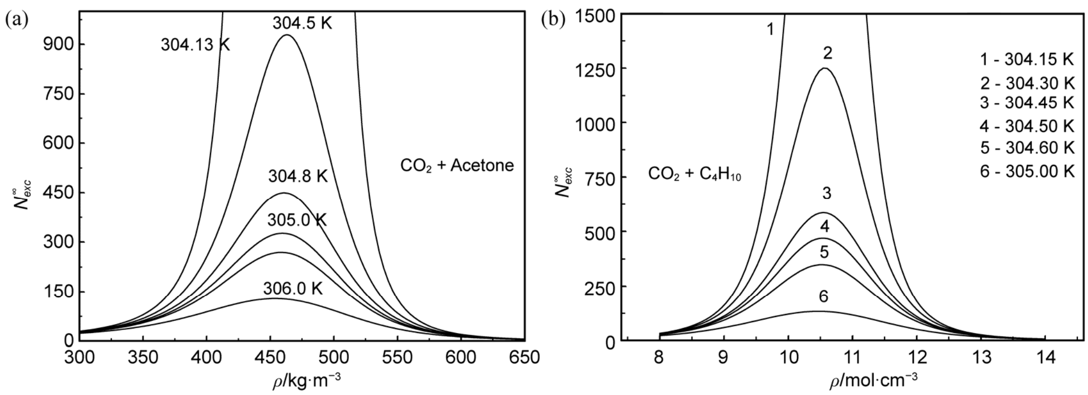

Fig. 35 Cluster's size, N^{∞}_{exc} as a function of density of pure solvent (CO_2) in binary mixture CO_2+Acetone and CO_2+n-C_4H_{10} along the supercritical isotherms calculated from Eq. (23) using crossover model [102,153-157].

($P\rho T$) surface and vapor-pressure (P_S–T_S) curve of fluids in the near- and supercritical regions. As Fig. 5 demonstrates, the sign of the $\left(\partial^2 P/\partial T^2\right)_\rho$ changes from positive (below ρ_C) to negative (above ρ_C) around the critical density (passing through the maximum near the critical point), depending on the supercritical isotherms. This means that C_V–ρ isotherms show the maximum around the critical density along the supercritical isotherms (see Fig. 5). As one can see from Eq. (24), the locus of C_V extreme, $\left(\partial C_V/\partial\rho\right)_T = 0$, coincides with a locus of P-T isochore inflection points, where $\left(\partial^2 P/\partial T^2\right)_\rho = \left(\partial C_V/\partial\rho\right)_T = 0$ [216-222]. The location of the C_V maxima or P–T inflection points in the supercritical region is changing with temperature (isotherm) increasing (see also our previous publication [216]). The loci of the isothermal and isochoric maxima and minima of heat capacity, $\left(\partial^2 P/\partial T^2\right)_\rho = \left(\partial C_V/\partial\rho\right)_T = 0$ and $\left(\partial C_V/\partial\rho\right)_\rho = 0$, for SC CO_2 are depicted in Figs. 36 to 38 in the P-T and ρ–T projections. Therefore, PVT data together with $C_V VT$ measurements are providing very useful theoretical information to develop functional form of the fundamental equation of state which is correctly taking into account non-classical (scaling), $C_V \propto \left(T - T_C\right)^{-\alpha}$, behavior of isochoric heat capacity and testing predictive capability of the various theoretical models. Thus, the asymptotic scaling behavior of the temperature dependence of pressure along the critical isochore near the critical point (in the sub- and supercritical regions) should be as $\Delta P\left(\rho_C, t\right) \propto t^{2-\alpha}$, (where α=0.11 is the universal critical exponent of the isochoric heat capacity), which means that the first temperature derivative of pressure

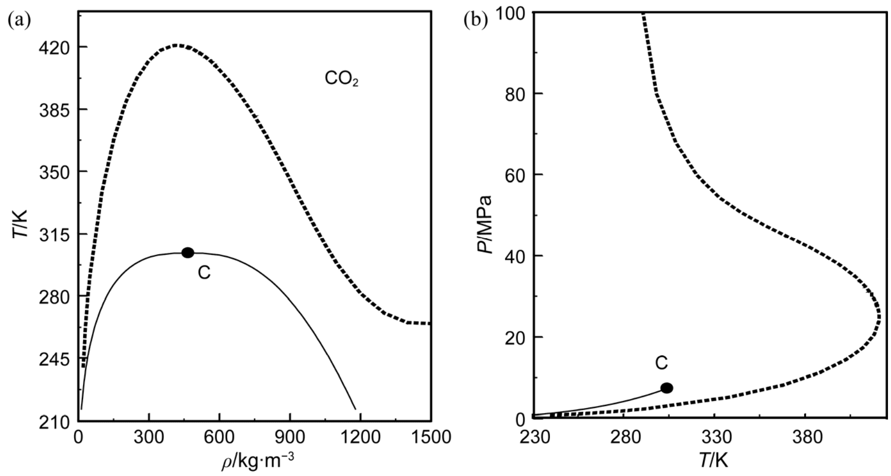

Fig. 36 Isochoric C_V minima $\left(\partial C_V/\partial T\right)_V = 0$ loci of CO_2 (dashed curves) in T–ρ and P–T projections. Solid curves are liquid+gas coexistence (a) and vapor-pressure curves (b) calculated from reference EOS [123] (REFPROP [124]).

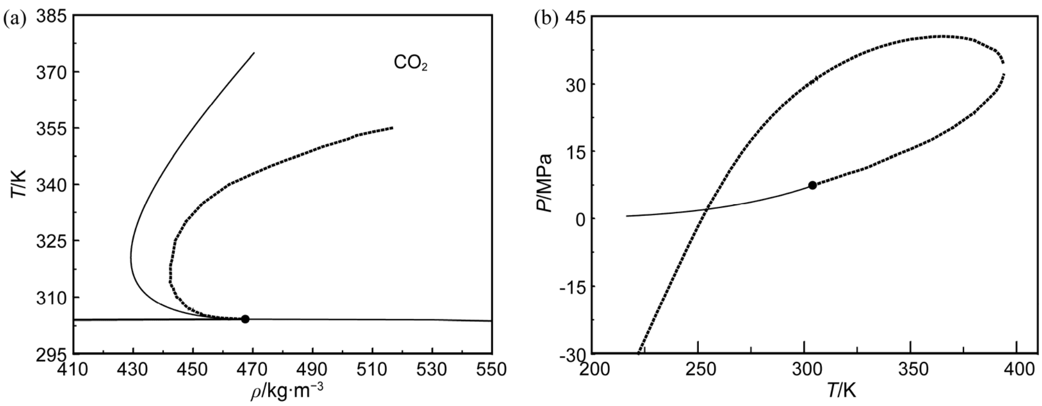

Fig. 37 Isothermal C_V maxima – minima, $\left(\partial C_V/\partial\rho\right)_T = 0$, loci or locus of P-T isochore inflection points, $\left(\partial^2 P/\partial T^2\right)_\rho = 0$, of CO_2 in T–ρ and P–T projections. Solid curves are liquid+gas coexistence curve (a) and vapor-pressure curves (b) calculated from reference EOS [123] (REFPROP [124]) and crossover model [153-157].

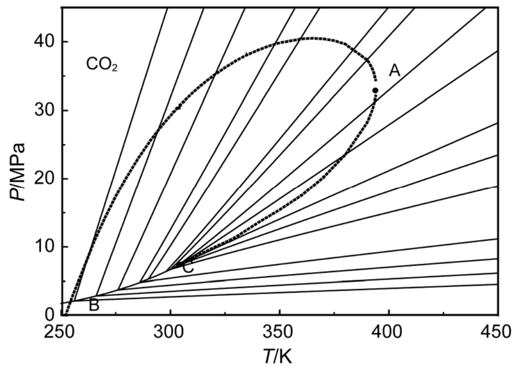

Fig. 38 Locus of isochore inflection points, $\left(\partial^2 P/\partial T^2\right)_\rho = 0$, in the *P-T* phase diagram of CO_2. Solid curves are *P-T* isochterms calculated from reference EOS [123] (REFPROP [124]). Dashed curve is the isochore inflection points calculated from isochoric heat capacity measurements, $\left(\partial C_V/\partial\rho\right)_T = 0$, by Abdulagatov et al. [216].

$\gamma_V = \left(\partial P/\partial T\right)_V$, remains finite at the critical point, while the second temperature derivative, $\left(\partial^2 P/\partial T^2\right)_{\rho c}$ and $\left(d^2 P_S/\partial T^2\right)$, diverges weakly as C_V, i.e., as $\propto t^{-\alpha}$. Both $\left(d^2 P_S/\partial T^2\right)$ and $\left(\partial^2 P/\partial T^2\right)_{\rho c}$ derived from C_V measurements goes to infinity at the critical point as $\propto t^{-\alpha}$ (scaling behavior). Therefore, the curvature parts of equation of state, $\Delta P(\rho, T)$, and vapor-pressure equation, $\Delta P_S(T)$, should be non- analytical function of the temperature at the critical point, for example

$$\Delta P_S(T) = P_1 t^{2-\alpha} + P_2 t^{2-\alpha+\Delta} + P_3 t^2 \quad (26)$$

where $t = (T - T_C)/T_C$ is the reduced temperature difference; T_C is the critical temperature; P_i (i = 1,3) are the adjustable parameters; Δ=0.52 is the universal critical exponent [227,228]. According to the complete scaling theory [229-233], the values of fitting parameters P_1 and P_3 in vapor-pressure Eq. (26) are related with the critical amplitude A_0^- and background parameter $\overline{B}_{cr}$ of the isochoric heat capacity (see Eqs. (27) and (28)),

$$\frac{C_V}{k_B} = A_0^- t^{-\alpha}\left(1 + A_1^- t^\Delta\right) - \frac{B_{cr}}{k_B} \quad (27)$$

and asymmetric parameter of the coexistence cure diameter a_3

$$\Delta\rho = \pm B_0 t^\beta \pm B_1 t^{\beta+\Delta} + B_2 t^{1-\alpha} - B_3 t + B_4 t^{2\beta} \quad (28)$$

where

$$B_2 = -b2\frac{A_0^-}{(1-\alpha)};\ B_3 = -b_2\frac{B_{cr}}{k_B},\ B_4 = \frac{a_3}{1-a3}B_0^2,\ as\ [120]$$

$$P_1 = \frac{A_0^-}{(1+a_3)(2-\alpha)(1-\alpha)},\ P_3 = \frac{1}{(1+a_3)} - \frac{1}{2}B_{cr} \quad (29)$$

Thus, isochoric heat capacity is providing very useful scientific information for study details of the supercritical fluids properties.

5. Asymptotic Critical Amplitudes of Carbon Dioxide

According to the scaling theory of critical phenomena [171,162-164], the thermodynamic properties of fluids near the critical point exhibit the same singular asymptotic critical behavior as that of a lattice-gas. Scaling theory correctly predicts the experimentally observed asymptotic thermodynamic behavior of fluids near the critical point as an asymptotical scaling power laws with universal critical exponents (α, β, γ, δ, ν) [121,171,162-164] and non-universal (system-dependent) critical amplitudes ($A_0^\pm$, B_0, D_0, $\Gamma_0^\pm$, ξ_0). The universality of scaling functions leads naturally to the universality of the critical amplitude combinations [115, 234-237]. According to the principle of universality of the critical phenomena (universality of the scaling functions), only two amplitudes ($A_0^\pm$, B_0, for example) are necessary to determine all other amplitudes such as ($D_0, \Gamma_0^\pm, \Gamma_0^-, \xi_0$). Both asymptotic critical amplitudes ($A_0^\pm$, B_0) can be determined form the same calorimetric (isochoric heat capacity) experiments (see details in [54,55,130-132,238]). Also, as shown above (Section 2.2.1, Eq. (9)), these asymptotic critical amplitudes ($A_0^\pm$, B_0) can be predicted using acentric factor, ω. Universal amplitude combinations are a key issue in the study of phase transitions and critical phenomena, and other related fields (supercritical phenomena, for example) and very important to study of the current status of theory and experiment. According to scaling theory (universality principle), the critical amplitude ratios ($\Gamma, A_0^+\Gamma_0^+B_0^2$, $D_0\Gamma_0^+B_0^{\delta-1}$, and Γ_0^+/Γ_0^-) are universal, depending only on universal critical exponents and associated with the universal scaling relations between the critical exponents. Universal critical exponents of isochoric heat capacity (α=0.11) and liquid-gas coexistence curve (β = 0.324) and their non-universal asymptotical critical amplitudes ($A_0^\pm$ and B_0) play an important role in theory of the critical phenomena and practical applications to develop scaling type equation of state for near-critical and supercritical fluids. For example, the asymptotic critical amplitudes ($A_0^\pm$ and B_0) together with other critical amplitudes (Γ_0^+ , D_0, ξ_0) satisfy to universal relations

[115-120,154,239] $A_0^+/A_0^- = 0.524$ [118,119], $\frac{\alpha A_0^+ \Gamma_0^+}{B_0^2} = 0.058$ [120,154], $D_0 \Gamma_0^+ B_0^{\delta-1} = 1.69$ [154,239], and $\xi_0 \left(\frac{\alpha A_0^+}{v_C} \right)^{1/3} = 0.266$ [115-117] (see also Table 1). The values of other critical amplitudes such as Γ_0^+, ξ_0 and D_0 can be estimated using these universal relations and the present values of the critical amplitudes for heat capacity ($\bar{A}_0$=7.95 [54], see Table 2 for CO_2) and coexistence curve ($\bar{B}_0$=1.64 [54]) for CO_2 as $\Gamma_0^+ = \frac{0.058 B_0^2}{\alpha A_0^+} = 0.18$, $D_0 = \frac{1.69}{\Gamma_0^+ B_0^{\delta-1}} = 1.40$, and $\xi_0 = 0.266 \left(\alpha A_0^+ v_C \right)^{-1/3} = 0.15$ nm, where v_C=$N_A \rho_C$ molecular volume at the critical point. The values of universal critical amplitude ratios predicted by various theoretical models [120,154,239,240] are presented in Table 2 together with the values derived from our experimental isochoric heat-capacity and coexistence curve data for CO_2 [54,55]. As one can see from Table 2, the agreement is good enough. The values of the asymptotic critical amplitudes (A_0^- and B_0) for CO_2 predicted from Eq. (9) using acentric factor ω are A_0^- =7.36 and B_0=1.72 (ω=0.22394 for CO_2). The uncertainties of the predicted values of (A_0^- and B_0) are 15% for A_0^- and 10% for B_0. These predicted data are deviated from our experimental values within 8% for A_0^- and 4.9% for B_0, i.e., close to their uncertainties. Also, the critical amplitude of the two-phase isochoric heat capacity (A_0^-), the background parameter $\bar{B}_{cr}$, and the asymmetric parameter a_3 of the coexistence curve can be used to estimate vapor-pressure equation parameters (P_1 and P_3) from Eq. (29). Thus, the values of the fitting parameters P_1 and P_3 of the vapor-pressure equation can be directly calculated from the asymptotic critical amplitudes (A_0^-, B_{cr}) of heat-capacity and asymmetric parameter a_3 of the coexistence curve singular diameter calculated from the measured isochoric heat- capacities and saturated densities for CO_2 [54,55,140-132]. This allows developing thermodynamically consistent equations for vapor pressure, saturated liquid and vapor densities, and two-phase heat-capacities, therefore, other thermodynamic properties.

Table 1 Experimental and theoretical universal critical amplitude ratios

Models	$\alpha A_0^+ \Gamma_0^+ B_0^{-2}$	$D_0 \Gamma_0^+ B_0^{\delta-1}$	A_0^+/A_0^-	Γ_0^+/Γ_0^-
Crossover model	0.052	1.64	0.524	4.96
ε expansion	0.048 [118]	1.67	0.520±0.01 [119]	4.90 [118]
d=3 field theory [240]	0.0594±0.0011	-	0.541±0.014	4.77±0.30
3D Ising model [119]	0.058±0.001	-	0.523±0.009	4.95±0.15
Experiment (this work, for benzene)	0.058	1.69	0.524	-

Table 2 Critical amplitudes for carbon dioxide

R_D	$\bar{T}_R$	ν	γ	$\bar{\Gamma}_0$	ξ_0/ nm	$\bar{q}_D^{-1}$ / nm	References
+1.01	2.0	0.63	1.2415	0.189	0.150	0.4	[170]
1.01	1.5	0.63	1.2415	0.189	0.150	0.4	[243]
T_C/ K	ρ_C/kmol·m^{-3}	P_C/MPa	$\bar{A}_0$	$\bar{B}_0$	$\bar{\Gamma}_0$	ξ_0/ nm	References
304.11	10.6	7.372	7.62	1.68	0.22	0.15	[241]
304.13	10.6	7.372	7.95	1.64	0.18	0.15	[54]
304.14	10.6	7.377	7.37	1.71	0.20	0.15	[242]

6. Conclusions

In the present review, we have provided comprehensive assessment of the available thermodynamic and transport properties of supercritical carbon dioxide and CO_2 containing binary mixtures, SC CO_2+solute, (experiment and theory) and their various technological and scientific applications in different natural and industrial processes. The existing crossover and reference multiparametric analytic equations of state for CO_2 (NIST REFPROP [124]) were analyzed to calculate the thermodynamic and transport properties of supercritical carbon dioxide. The critical properties data (critical lines) of the SC CO_2 containing binary mixtures were used to estimate the value of the Krichevskii parameters for CO_2+solute near the critical point of pure CO_2. The role of the critical line shapes of the carbon dioxide containing binary mixtures SC CO_2+solute in determination of the critical thermodynamic behavior of the dilute mixture near the critical point of pure CO_2 using the Krichevskii parameter concept were studied. Calculation of the critical anomalies of the thermodynamic properties (solubility, Henry's constant, partial molar properties) using the Krichevskii parameter near the critical point of pure CO_2 were detailed reviewed. Simplified scaling type equation based on mode-coupling theory of critical dynamics with two critical amplitudes ($\overline{A}_0$ and $\overline{B}_0$) and one cutoff wave number ($\overline{q}_D$) as fluid-specific parameters can be used to accurately predict the transport properties (thermal conductivity, viscosity and thermal diffusivity) of supercritical carbon dioxide. The recommended values of the specific parameters (asymptotic critical amplitudes, $\overline{A}_0$, $\overline{B}_0$, D_0, Γ_0^+, Γ_0^-, and ξ_0) of the carbon dioxide for practical and scientific use were provided.

Acknowledgment

This work was supported by Russian Foundation of Basic Research (RFBR) grants № 19-08-00056 and №18-08-00500.

References

[1] Pruess K., Azaroual M., On the feasibility of using supercritical CO_2 as heat transmission fluid in an engineered hot dry rock geothermal system. In: Proceedings 31th Workshop on Geothermal Reservoir Engineering Stanford University, Stanford, California, 2006.

[2] Brown D.W., A hot dry rock geothermal energy concept utilizing supercritical CO_2 instead of water. In: Proceedings Twenty-Fifth Workshop on Geothermal Reservoir Engineering Stanford University, Stanford, California, 2000.

[3] Huang C.J., Hsieh J.C., Lin D.T., The experimental study of heat extraction of supercritical CO_2 in the geothermal reservoir. MATEC Web of Conferences. - EDP Sciences, 2016, 60: 04010.

[4] He Y., Bai B., Li X., Numerical study on the heat transfer characteristics of supercritical water in a rock fracture for enhanced geothermal systems. International Journal of Thermophysics, 2018, in press.

[5] Supercritical CO_2 Power Cycle Symposium, The Power Industry's Next Phase Shift, May 24–25, 2011, U.S. Department of Energy, Boulder, CO USA.

[6] Pan L., Freifeld B., Doughty C., et al., Fully coupled wellbore-reservoir modeling of geothermal heat extraction using CO_2 as the working fluid. Geothermics, 2015, 53: 100–113.

[7] Atrens A.D., Gurgenci H., Rudolph V., Electricity generation using a carbon-dioxide thermosiphon. Geothermics, 2010, 39(2): 161–169.

[8] Xu T., Feng G., Shi Y., On fluid-rock chemical interaction in CO_2-based geothermal systems. Journal of Geochemical Exploration, 2014, 144: 179–193.

[9] Hsieh J.C., The heat extraction investigation of supercritical carbon dioxide flow in heated porous media. Energy Procedia, 2014, 61: 262–265.

[10] Liu L., Suto Y., Bignall G., CO_2 injection to granite and sandstone in experimental rock/hot water systems. Energy Conversion and Management, 2003, 44(9): 1399–1410.

[11] Buscheck T.A., Bielicki J.M., Chen M., Integrating CO_2 storage with geothermal resources for dispatchable renewable electricity. Energy Procedia, 2014, 63: 7619–7630.

[12] Randolph J.B., Saar M.O., Bielicki J., Geothermal energy production at geologic CO_2 sequestration sites: Impact of thermal drawdown on reservoir pressure. Energy Procedia, 2013, 37: 6625–6635.

[13] Jiang P.X., et al., Convection heat transfer of supercritical pressure carbon dioxide in a vertical micro tube from transition to turbulent flow regime. International Journal of Heat and Mass Transfer, 2013, 56(1): 741–749.

[14] Liu G., et al., Effect of buoyancy and flow acceleration on heat transfer of supercritical CO_2 in natural circulation loop. International Journal of Heat and Mass Transfer, 2015, 91: 640–646.

[15] Herzog H.J., Peer reviewed: what future for carbon capture and sequestration? Environmental Science & Technology, 2001, 35: 148A–153A.

[16] Benson S.M., Cole D.R., CO_2 sequestration in deep sedimentary formations. Elements, 2008, 4(5): 325–331.

[17] Harvey O.R., et al., Geochemical implications of gas leakage associated with geologic CO_2 storage-A qualitative review. Environmental Science & Technology, 2012, 47(1): 23–36.

[18] Bachu S., Adams J.J., Sequestration of CO_2 in geological media in response to climate change: capacity of deep saline aquifers to sequester CO_2 in solution. Energy Conversion and Management, 2003, 44(20): 3151–3175.

[19] White C.M., et al., Sequestration of carbon dioxide in coal with enhanced coalbed methane recovery a review. Energy & Fuels, 2005, 19(3): 659–724.

[20] Streit J.E., Hillis R.R., Estimating fault stability and sustainable fluid pressures for underground storage of CO_2 in porous rock. Energy, 2004, 29 (9-10): 1445–1456.

[21] Hendriks C.A., Blok K., Underground storage of carbon dioxide. Energy Conversion and Management, 1993, 34 (9-11): 949–957.

[22] Bachu S., Sequestration of CO_2 in geological media: criteria and approach for site selection in response to climate change. Energy Conversion and Management, 2000, 41: 953–970.

[23] Kaupp G., Reactions in supercritical carbon dioxide. Angewandte Chemie International Edition in English, 1994, 33: 1452–1455.

[24] Savage P.E., et al., Reactions at supercritical conditions: applications and fundamentals. American Institute of Chemical Engineering Journal, 1995, 41: 1723–1778.

[25] Clifford T., Bartle K., Chemical reactions in supercritical fluids. Chemical Industry, 1996, 17: 449–469.

[26] Abbasov Z.Y., Fataliev V.F., About the physical nature of the retrograde condensation pressure of gas-condansate systems in the porous media condition. In: Proc. Azerbaidjan Academy of Sciences, Section Sciences of Earth, 2015, 3: 60–66.

[27] Katz D.L., Kurata F., Retrograde condensation. Industrial & Engineering Chemistry, 1940, 32: 817–827.

[28] Raghavan R., Jones J.R., Depletion performance of gas-condensate reservoirs. Journal of Petroleum Technology, 1996, 48(08): 725–31.

[29] Anton K., From potential to practice: relevant industrial applications of packed-column supercritical fluid chromatography. Journal of Chromatographic Science, 1994, 32(10): 430–438.

[30] Schneider G.M., Applications of fluid mixtures and supercritical solvents: A survey. Supercritical Fluids. - Springer, Dordrecht, 1994, pp.: 739–757.

[31] McHugh M., Krukonis V., Supercritical fluid extraction. Butterworths, London, 1986, pp.: 507.

[32] Schneider G.M., Stahl E., Wilke G. (ed.). Extraction with supercritical gases. Weinheim, Verlag Chemie, 1980, pp.:189.

[33] Schneider G.M., Survey on applications of fluid mixtures and supercritical solvents presented at this meeting. In: Proceeding of the International Symposium on Supercritical Fluids. M. Perrut, (ed.), Nice, France, 1988, pp.: 1–17.

[34] Salto S., Research activities on supercritical fluid science and technology in Japan-a review. The Journal of Supercritical Fluids, 1995, 8(3): 177–204.

[35] Lauer H.H., McManigill D., Board R.D., Mobile-phase transport properties of liquefied gases in near critical and supercritical fluid chromatography. Analytical Chemistry, 1983, 55(8): 1370–1375.

[36] Wasen U., Swaid I., Schneider G.M., Physicochemical principles and applications of supercritical fluid chromatography (SFC). New analytical methods (19), Angewandte Chemie International Edition in English, 1980, 19(8): 575–587.

[37] Wilson I.D., Davis P., Ruane R.J., Supercritical fluid chromatography and extraction of pharmaceuticals. In: Application of Supercritical Fluids in Industrial Analysis. J.R. Dean, (ed.), CRC Press Inc., Boca Raton, FL, 1993, pp.74–104.

[38] Schneider, G.M., High-pressure investigations of fluid mixtures-review and recent results. Journal of Supercritical Fluids, 1998, 13: 5–14.

[39] Kiran E., Levelt Sengers J.M.H., (eds.), Supercritical fluids fundamentals for application, NATO, ASI Ser. 1993, Vol. 273.

[40] Kiran E., Brennecke J.F., (eds.), Supercritical fluid engineering science, ACS, Symp. Ser. 514, Washington, D.C., 1993.

[41] Manssori G.A., Savidge J.L., Predicting retrograde phenomena and miscibility using equation of state. SPE 19809, SPE, Inc., 1989, pp.: 383–398.

[42] Orr F.M. Jr., Taber J.J., Displacement of oil by carbon dioxide. Annual Report to the USA DOE Report No. DOE/BC/10331-4, 1981.

[43] Larson L.L., Temperature dependence of L1/L2/V behavior in CO_2/hydrocarbon systems. SPE Reservoir Engineering, 1989, 4: 105–114.

[44] Voulgaris M.E., Peters C.J., de Swaan Arons J., On the retrograde condensation behavior of lean natural gas. International Journal of Thermophysics, 1995, 16(3): 629–642.

[45] Standing M.B., Volumetric and phase behavior of oil field hydrocarbon systems. Millet the Printer, Inc., Dallas, TX, 1977.

[46] Orr Jr F.M., et al., Equilibrium phase compositions of CO2/crude oil mixtures-part 2: comparison of continuous multiple-contact and slim-tube displacement tests. Society of Petroleum Engineers Journal, 1983, 23(02): 281–291.

[47] Doscher, T.M., El-Arabi M., Scaled model experiments show how CO_2 might economically recover residual oil. Oil Gas Journal, 1982, 80: 144–151.

[48] Holm L.R.W., et al., Effect of oil composition on miscible-type displacement by carbon dioxide. Society of Petroleum Engineers Journal, 1982, 22(01): 87–98.

[49] Stalkup F.I., Status of miscible displacement. Journal of Petroleum Technology, 1983, 1: 815–827.

[50] Dadashev M.N., Abdulagatov A.I., Experimental study of the process of extraction with carbon dioxide in the supercritical conditions. Russian Journal of Chemistry and Chemical Production, 1997, 3(4): 64–79.

[51] Polikhronidi N.G., Batyrova R.G., Abdulagatov I.M., at al., Isochoric heat capacity measurements for a CO_2+n-decane mixture in the near-critical and supercritical regions. Journal of Supercritical Fluids, 2004, 33: 209–222.

[52] Polikhronidi N.G., Batyrova R.G., Abdulagatov I.M., et al., Isochoric Heat Capacity of CO_2 + n-Decane Mixtures in the Critical Region. International Journal of Thermophysics, 2006, 27: 729–759.

[53] Abdulagatov I.M., Polikhronidi N.G., Batyrova R.G., *PVTx* and thermal-pressure coefficient measurements of the binary CO_2+ n-decane mixtures in the critical and retrograde regions. The Journal of Chemical Thermodynamics, 2018, 125: 107–135.

[54] Abdulagatov I.M., Polikhronidi N.G., Batyrova R.G., Measurements of the heat capacities C_V of carbon dioxide in the critical region. The Journal of Chemical Thermodynamics, 1994, 26: 1031–1045.

[55] Abdulagatov I.M., Polikhronidi N.G., Batyrova R.G., Isochoric heat capacity and liquid-gas coexistence curve of carbon dioxide in the region of the immediate vicinity of the critical point. Berichte der Bunsengesellschaft für physikalische Chemie, 1994, 98: 1068–1072.

[56] Dixon D.J., Johnston K.P., Supercritical fluids, Encyclopedia of Chemical Technology, 4th ed., 1997, 23: 452.

[57] Wang S., Kienzle F., The syntheses of pharmaceutical intermediates in supercritical fluids. Industrial & Engineering Chemistry Research, 2000, 39(12): 4487–4490.

[58] Brennecke, J.F., New applications of supercritical fluids. Chemistry and Industry, 1996, 21: 831–834.

[59] Lenhard U., Luerken F., Boeckler T., Donnerhacu A., CO_2-extractions. Process Design and Economics, Food Marketing & Technology, 1990, 5: 56.

[60] Tom J.W., Lim G.B., Debenedetti P.G., Prud'homme R.K., Applications of supercritical fluids in the controlled release of drugs. American Chemical Society Symposium Series, 1993, 514: 238–257.

[61] Yeo S.D., Formation of microparticulate protein powder using a supercritical fluid antisolvent. Biotechnology and Bioengineering, 1993, 41(3): 341–346.

[62] Winters M.A., et al., Precipitation of proteins in supercritical carbon dioxide. Journal of Pharmaceutical Sciences, 1996, 85(6): 586–594.

[63] Kutson B.L., Debenedetti P.G., Tom J.W., Microparticulate systems for the delivery of proteins and vaccines. Cohen S., Brenstein H., (eds.), Marcel Dekker Inc., New York, 1998.

[64] Roston D.A., Sun J.J., Supercritical fluid extraction method development for extraction of an experimental HIV protease inhibitor drug from animal feed. Journal of Pharmaceutical and Biomedical Analysis, 1997, 15(4): 461–468.

[65] Subramaniam B., Rajewski R.A., Snavely K., Pharmaceutical processing with supercritical carbon dioxide. Journal of Pharmaceutical Sciences, 1997, 86: 885–890.

[66] Groves Jr F.R., State of the art on the supercritical extraction of organics from hazardous wastes. Critical Reviews in Environmental Science and Technology, 1985, 15: 237–274.

[67] Akgerman A., Roop R.K., Hess R.K., Yeo S.D., Environmental application of supercritical extraction. In: Supercritical Fluid Technology: Reviews in Modern Theory and Applications. T.J. Bruno, J.F. Ely, (eds.), CRC Press, Boca Raton, FL, 1991, Chapter 14.

[68] De Fillipi R.P., Krukonis V.J., Model M., Supercritical fluid regeneration of activated carbon for absorption of pesticides. Environmental Protection Agency Report, No. EPA-60012-80-054, 1980.

[69] Eppig C.P., De Fillipi R.P., Murphy R.A. Supercritical fluid regeneration o f activated carbon as having a 13C CP-MAS aromaticity value of about 0.22. U.S. EPA Report 600/2-82-067, EPA Office of Research and Development, Research Triangler Park, NC, 1981.

[70] Ringhasnd P.H., Kopfler F.C. Isolation and concentration of organic substances from water an evaluation of supercritical fluid extraction. 186th National Meeting of the ACS, Washington, DC, August 28 to September 3, 1983.

[71] Laitinen A., Michaux A., Aaltonen O., Soil cleaning by carbon dioxide extraction: a review. Environmental Technology, 1994, 15: 715–727.

[72] Hess R.K., Erkey C., Akgerman A., Supercritical extraction of phenol from soil. The Journal of Supercritical Fluids, 1991, 4: 47–52.

[73] Hawthorne S.B., Miller D.J., Extraction and recovery of polycyclic aromatic hydrocarbons from environmental solids using supercritical fluids. Analytical Chemistry, 1987, 59(13): 1705–1708.

[74] Janda V., Bartle K., Clifford A.A., Supercritical fluid extraction in environmental analysis. In: Application of Supercritical Fluids in Industrial Analysis, J.R. Dean, (ed.), CRC Press Inc., Boca Raton, FL, 1993: 159–188.

[75] Orr F.M., Sliva M.K., Lien C.L., Equilibrium phase compositions of CO/sub 2//hydrocarbon mixtures-part 1: Measurement by a continuous multiple-contact experiment. Society of Petroleum Engineers Journal, 1982, 22: 272–280.

[76] Holm L.W., Josendal V.A., Effect of oil composition on miscible-type displacement by carbon dioxide. Society of Petroleum Engineers Journal, 1982, 22: 87–98.

[77] Dadashev M.N., Abdulagatov A.I., Experimental study of the process of extraction with carbon dioxide in the supercritical conditions. Russian Journal of Chemistry and Chemical Production, 1997, 3: 64–69.

[78] Dadashev M.N., Abdulagatov A.I., Supercritical extraction of vegetable products. Russian Journal of Chemical Production, 1997, 5: 35–40.

[79] Caragay A.B., Little A.D., Supercritical fluids for

extraction of flavors and fragrances from natural products. Parfumer & Flavorist, 1981, 6: 43–54.

[80] Papamichail I., Louli V., Magoulas, K., Supercritical fluid extraction of celery seed oil. Journal of Supercritical Fluids, 2000, 18: 213–226.

[81] Berna A., Tarrega A., Blasco M., Subirats S., Supercritical CO_2 extraction of essential oil from orange peel; effect of the height of the bed. Journal of Supercritical Fluids, 2000, 18: 227–237.

[82] Subramanyam C.V., Use of supercritical fluids in vegetable oil industries. Chemical Engineering World, 1989, 24: 35–39.

[83] Moyler D.A., Extraction of flavours and fragrances with compressed CO_2. In: Extraction of Natural Products Using Near-Critical Solvents. M.B. King, T.R. Bott, (eds.), Glasgow: Chapman & Hall, 1993, pp.: 140-183.

[84] Ting S.S.T., Macnaughton S.J., Tomasko D.L., Foster N.R., Solubility of naproxen in supercritical carbon dioxide with and without cosolvents. Industrial & Engineering Chemical Research, 1993, 32: 1471–1481.

[85] Gurdial G.S., Macnaughton S.J., Tomasko D.L., Foster N.R., Influence of chemical modifiers on the solubility of o- and m-hydroxybenzoic acid in supercritical carbon dioxide. Industrial & Engineering Chemical Research, 1993, 32: 1488–1497.

[86] Dobbs J.M., Wong J.M., Lahiere R.J., Johnston K.P., Modification of supercritical fluid phase behavior using polar cosolvents. Industrial & Engineering Chemical Research, 1987, 26: 56–65.

[87] Ekart M.P., Bennett K.L., Ekart S.M., et al., Cosolvent interactions in supercritical fluid solutions. American Institute of Chemical Engineering Journal, 1993, 39: 235–248.

[88] Dooley K.M., Kao Ch.P., Gambrell R.P., Knopf, F.C., The use of entrainers in the supercritical extraction of soils contaminated with hazardous organics. Industrial & Engineering Chemical Research, 1987, 26: 2058–2062.

[89] Schmitt W.J., Reid R.C., The use of entrainers in modifying the solubility of phenanthrene and benzonic acid in supercritical carbon dioxide and ethane. Fluid Phase Equilibria, 1986, 32: 77–99.

[90] Dobbs J.M., Wong J.M., Johnston J.P., Nonpolar cosolvents for solubility enhancement in supercritical fluid carbon dioxide. Journal of Chemical and Engineering Data, 1986, 31: 303–308.

[91] Dobbs J.M., Johnston J.P., Selectivities in pure and mixed supercritical fluid solvents. Industrial & Engineering Chemical Research, 1987, 26: 1476–1482.

[92] Gurdial G.S., Foster N.R., Yun S.L.J., Tilly K.D.T., Phase behavior of supercritical fluid-entrainer systems, In: Symposium on Supercritical Fluids. Annual AIChE Meeting, Los Angeles, 17-22 November, 1991, pp.: 34–45.

[93] Levelt Sengers J.M.H., Morrison G., Nielson G., Thermodynamic behavior of supercritical fluid mixtures. International Journal of Thermophysics, 1986, 7: 231–243.

[94] Chang R.F., Morrison G., Levelt Sengers J.M.H., The critical dilemma of dilute mixtures. The Journal of Physical Chemistry, 1984, 88: 3389–3391.

[95] Levelt Sengers J.M.H., Solubility near the solvent's critical point. Journal of Supercritical Fluids, 1991, 4: 215–222.

[96] Harvey A. H., Levelt Sengers J.M.H., Unified description of infinite-dilution thermodynamic properties of aqueous solutions. The Journal of Physical Chemistry, 1991, 95: 932–937.

[97] Levelt Sengers J.M.H., Thermodynamics of solutions near the solvent's critical point. In: Supercritical Fluid Technology, J.F. Ely, T.J. Bruno,(eds.), CRC Press, Boca Raton, FL, 1991, pp.: 1–50.

[98] Chang R.F., Levelt Sengers J.M.H., Behavior of dilute mixtures near the solvent's critical point. The Journal of Physical Chemistry, 1986, 90: 5921–2927.

[99] Kiselev S.B., Sengers J.V., An improved parametric crossover model for the thermodynamic properties of fluids in the critical region. International Journal of Thermophysics, 1993, 14: 1–32.

[100] Kiselev S.B., Abdulagatov I.M., Harvey A.H., Equation of state and thermodynamic properties of pure D_2O and D_2O+H_2O mixtures in and beyond the critical region. International Journal of Thermophysics, 1999, 20: 563–588.

[101] Kiselev S.B., Ely J., Abdulagatov I.M., Bazaev A.R., Magee J.W., Equation of state and thermodynamic properties of pure toluene and dilute aqueous toluene solutions in the critical and supercritical regions. Industrial & Engineering Chemical Research, 2002, 41: 1000–1016.

[102] Kiselev S.B., Rainwater J.C., Enthalpies, excess volumes, and specific heats of critical and supercritical binary mixtures. The Journal of Chemical Physics, 1998, 109: 643–657.

[103] Kiselev S.B., Prediction of the thermodynamic properties and the phase behavior of binary mixtures in the extended critical region. Fluid Phase Equilibria, 1997, 128: 1–28.

[104] Kiselev S.B., Ely J.F., Generalized corresponding states model for bulk and interfacial properties in pure fluids and fluid mixtures. The Journal of Chemical Physics, 2003, 119: 8645–8662.

[105] Kiselev S.B., Cubic crossover equation of state. Fluid Phase Equilibrium, 1998, 147: 7–23.

[106] Kiselev S.B., Ely J.F., Simplified crossover SAFT equation of state for pure fluids and fluid mixtures. Fluid Phase Equilibrium, 2000, 174(1–2): 93–113.

[107] Abdulagatov I.M., Bazaev A.R., Magee J.W., et al., *PVTx*

Measurements and crossover equation of state of pure *n*-hexane and dilute aqueous n-hexane solutions in the critical and supercritical regions. Industrial & Engineering Chemical Research, 2005, 44: 1967–1984.
[108] Anisimov M.A., Kiselev S.B., Sengers J.V., Tang S., Crossover approach to global critical phenomena in fluids. Physica, 1992, A 188: 487–525.
[109] Belyakov M.Yu., Kiselev S.B., Rainwater J.C., Crossover Leung-Griffiths model and the phase behavior of binary mixtures with and without chemical reaction. Fluid Phase Equilibria, 1998, 151-152: 439–449.
[110] Belyakov M.Yu., Kiselev S.B., Rainwater J.C., Crossover Leung-Griffiths model and the phase behavior of dilute aqueous ionic solutions. The Journal of Chemical Physics, 1997, 107: 3085–3097.
[111] Povodyrov A.A., Jin G.X., Kiselev S.B., Sengers J.V., Crossover equation of state for the thermodynamic properties of mixtures of methane and ethane in the critical region. International Journal of Thermophysics, 1996, 17: 909–944.
[112] Teja A.S., Smith R.L., The correlation and prediction of critical states of mixtures using a corresponding states principle. In: Chemical Engineering at Supercritical Conditions, M.E. Paulitis, R.D. Gray, T. Penninger, P. Davidson, (eds.), Ann Arbor Science. 1983, Chapter 15: 341–357.
[113] Jones I.W., Rowlinson J.S., Gas-liquid critical temperatures of binary mixtures. Transactions of the Faraday Society, 1963, 59: 1702–1708.
[114] van Konynenburg P.H., Scott R.L., Critical lines and phase equilibria in binary van der Waals mixtures. Philosophical Transactions of the Royal Society, 1980, 298*:* 495–540.
[115] Privman V., Hohenberg P.C., Aharony A., Phase transitions and critical phenomena. Domb C., Lebowitz L., (ed.), AP, NY, 1999, 14: 1–367.
[116] Pelissetto A., Vicari E., Critical phenomena and renormalization-group theory. Physics Reports, 2002, 368(6): 549–727.
[117] Fisher M.E., Zinn Sh.-Y., The shape of the van der Waals loop and universal critical amplitude ratios. Journal of Physics A, 1998, 319: L629–L635.
[118] Nicoll J.F., Albright P.C., Crossover functions by renormalization-group matching: three-loop results. Physical Review B, 1985, 31(7): 4576-4589.
[119] Bervillier C., Estimate of a universal critical-amplitude ratio from its ε expansion up to ε 2. Physical Review B, 1986, 34(11): 8141-8143.
[120] Behnejad H., Sengers J.V., Anisimov M.A., Thermodynamic behavior of fluids near the critical points. In: Applied Thermodynamics Fluids, A.R.H. Goodwin, J.V. Sengers, C.J. Peters, (eds.), IUPAC, 2010, Chapter 10, pp.: 321–367.
[121] Perkins R.A., Sengers J.V., Abdulagatov I.M., Huber M.L., Simplified model for the critical thermal-conductivity enhancement in molecular fluids. International Journal of Thermophysics, 2013, 34: 191–212.
[122] Sengers J.V., Effect of critical fluctuations on the thermodynamic and transport properties of supercritical fluids. In: Supercriticaal Fluids, Kiran E. and Levelt Sengers J.M.H. (eds.), Kulwer Acad. Publ., The Nitherlands, 1994, pp.: 231–271.
[123] Span, R., Wagner, W., Equations of state for technical applications. III. Results for polar fluids. International Journal of Thermophysics, 2003, 24(1): 111–162.
[124] Lemmon E.W., Huber M.L., McLinden M.O., NIST Standard Reference Database 23, NIST Reference Fluid Thermodynamic and Transport Properties, REFPROP, version 10.1, Standard Reference Data Program, National Institute of Standards and Technology, Gaithersburg, MD. 2018.
[125] Frenkel M., Chirico R., Diky V., Muzny C.D., Kazakov A.F., Magee J.W., Abdulagatov I.M., Jeong Won Kang: NIST Thermo Data Engine, NIST Standard Reference Database 103b-Pure Compound, Binary Mixtures, and Chemical Reactions, Version 5.0, National Institute Standards and Technology, Boulder, Colorado-Gaithersburg, MD, 2010.
[126] Dordain L., Coxam J.Y., Quint J.R., et al., Isobaric heat capacities of carbon dioxide and argon between 323 and 423 K and at pressures up to 25 MPa. Journal of Supercritical Fluids, 1995, 8: 228–235.
[127] Rivkin S.L., Gukov V.M., Isobaric heat capacity of carbon dioxide containing impurities at supercritical pressures. Teploenergetika, 1971, 18: 82–83.
[128] Koppel L. B., Smith J. M., Thermal properties of carbon dioxide in the critical region. Journal of Chemical Engineering Data, 1960, 5: 437–440.
[129] Boulton J. R., Stein F. P., The constant pressure heat capacity of supercritical carbon dioxide-methanol and carbon dioxide-ethanol cosolvent mixtures. Fluid Phase Equilibria, 1993, 91: 159–176.
[130] Amirkhanov Kh.I., Polikhronidi, N.G., Alibekov B.G., Batyrova R.G., Isochoric heat capacity c(v) of carbon dioxide. Teploenergetika, 1971, 18: 59–62.
[131] Amirkhanov Kh.I., Polikhronidi N.G., Batyrova R.G., Experimental determination of the specific heat of liquid carbon dioxide. Teploenergetika, 1970, 17: 70–72.
[132] Magee J.W., Ely J.F., Specific heats (C v) of saturated and compressed liquid and vapor carbon dioxide. International Journal of Thermophysics, 1986, 7(6): 1163–1182.
[133] Haase R., Tillmann W., Heat capacities of one-component and two-component fluid systems in the critical region. Zeitschrift für Physikalische Chemie,

1994, 187(2): 317–317.
[134] Beck L., Ernst G., Gurtner J., Isochoric heat capacity *C*v of carbon dioxide and sulfur hexafluoride in the critical region. Journal of Chemical Thermodynamics, 2002, 34: 277–292.
[135] Ernst G., Gurtner J., Beck L.A., *C*v calorimeter of small dimension. Journal of Chemical Thermodynamics, 1997, 29: 1189–1203.
[136] Zhang X., Zhang X., Han B., at al., Determination of constant volume heat capacity of mixed supercritical fluids and study on the intermolecular interaction. Journal of Supercritical Fluids, 2002, 24: 193–201.
[137] Estrada-Alexanders A. F., Trusler J. P.M. Speed of sound in carbon dioxide at temperatures between (220 and 450) K and pressures up to 14 MPa. The Journal of Chemical Thermodynamics, 1998, 30: 1589–1601.
[138] Liu Q., Feng X., An B., Duan Y., Speed of sound measurements using a cylindrical resonator for gaseous carbon dioxide and propene. Journal of Chemical Engineering Data, 2014, 59: 2788–2798.
[139] Kestin J., Khalifa H.E., Wakeham W.A., Viscosity of multicomponent mixtures of four complex gases. The Journal of Chemical Physics, 1976, 65: 5186–5188.
[140] Timrot D.L., Traktueva S.A., Dependence of the viscosity of CO_2 and SF_6 on temperature at moderate densities. High Temperature (Engl. Transl.), 1975, 22: 105–108.
[141] Estrada-Alexanders A.F., Hurly J.J., Kinematic viscosity and speed of sound in gaseous CO, CO_2, SiF_4, SF_6, $C4F_8$, and NH_3 from 220 K to 375 K and pressures up to 3.4 MPa. The Journal of Chemical Thermodynamics, 2008, 40: 193–202.
[142] Hunter I.N., Marsh G., Matthews G.P., Smith E.B., Argon + carbon dioxide gaseous mixture viscosities and anisotropic pair potential energy functions. International Journal of Thermophysics, 1993, 14: 819–833.
[143] Michels A., Sengers J.V., Van der Gulik P.S., The thermal conductivity of carbon dioxide in the critical region. Physica, 1962, 28: 1216–1237.
[144] Le Neindre B., Bury P., Tufeu R., Recent developments at bellevue on thermal conductivity measurements of compressed gases thermal conductivity. Proceeding of the Seventh Thermophysicaal Conference 1968, Gaithersburg Maryland, November 13, pp.: 579–593.
[145] LeNeindre B., Contribution to the experimental study of the thermal conductivity of some high temperature and high pressure fluids. International Journal of Heat and Mass Transfer, 1972, 15: 1–24.
[146] LeNeindre B., Tufeu R., Bury P., Sengers J.V., Thermal conductivity of carbon dioxide and steam in supercritical region. Berichte der Bunsengesellschaft für Physikalische Chemie, 1973, 77: 262–275.
[147] LeNeindre B., Bury P., Tufeu R., Johannin P., Vodar B., The thermal conductivity of carbon dioxide at high temperatures and high pressures. Shanks, H. R. (ed.), U. S. Atomic Energy Commission, 9th Conference on Thermal Conductivity, 1969.
[148] Span R., Wagner W., A New Equation of State for Carbon Dioxide Covering the Fluid Region from the Triple-Point Temperature to 1100 K at Pressures up to 800 MPa. Journal of Physical and Chemical Reference Data, 1996, 25(6):1509–1596.
[149] Huber M.L., et al. Reference correlation of the thermal conductivity of carbon dioxide from the triple point to 1100 K and up to 200 MPa. Journal of Physical and Chemical Reference Data, 2016, 5(1): 013102.
[150] Laesecke A., Muzny C.D., Reference correlation for the viscosity of carbon dioxide. Journal of Physical and Chemical Reference Data, 2017, 46: 013107.
[151] Quinones-Cisneros S.E., Deiters U.K., Generalization of the friction theory for viscosity modeling. Journal of Physics and Chemistry B, 2006, 110(25): 12820–12834.
[152] Fenghour A., Wakeham W.A., Vesovic V., The viscosity of carbon dioxide. Journal of Physical and Chemical Reference Data, 1998, 27: 31–44.
[153] Kiselev S.B., Friend D.G., Revision of a multiparameter equation of state to improve the representation in the critical region: application to water. Fluid Phase Equilibria, 1999, 155: 33–55.
[154] Kiselev S.B., Sengers J.V. An improved parametric crossover model for the thermodynamic properties of fluids in the critical region. International Journal of Thermophysics, 1993, 14: 1–32.
[155] Kiselev S.B., Huber M.L., Transport properties of carbon dioxide-ethane and methane+ethane mixtures in the extended critical region. Fluid Phase Equilibria, 1998, 142: 253–280.
[156] Kiselev S. B. Prediction of the thermodynamic properties and the phase behavior of binary mixtures in the extended critical region. Fluid Phase Equilibria, 1997, 128(1–2): 1-28.
[157] Kiselev S.B., Rainwater J.C., Huber M.L., Binary mixtures in and beyond the critical region: Thermodynamic properties. Fluid Phase Equilibria, 1998, 150: 469–478.
[158] Adamov Sh.P., Anisimov M.A., Smirnov V.A., Experimental study of the isochoric heat capacity of binary mixture of argon+carbon dioxide. In: Thermophysical Properties of Substances and Materials. GSSSD, Moscow, 1983, 18: 13–19.
[159] Adamov Sh.P., Anisimov M.A., Smirnov V.A., Experimental study of the isochoric heat capacity of carbon dioxide over the wide range of the critical point. In: Thermophysical Properties of Substances and Materials. GSSSD, Moscow, 1983, 18: 7–13.
[160] Herget C.M., Ultrasonic velocity in carbon dioxide and ethylene in the critical region. The Journal of Chemical

Physics, 1940, 8(7): 537–542.
[161] Estrada-Alexanders A.F., Trusler J.P.M., Speed of sound in carbon dioxide at temperatures between (220 and 450) K and pressures up to 14 MPa. The Journal of Chemical Thermodynamics, 1998, 30: 1589–1601.
[162] Fisher M.E., The renormalization group in the theory of critical behavior. Reviews of Modern Physics, 1974, 46: 597-616.
[163] Wilson K.G., The renormalization group: Critical phenomena and the Kondo problem. Reviews of Modern Physics, 1975, 47: 773-840.
[164] Fisher M.E., Critical phenomena, lectures notes in Physics. F.J.W. Hahne, (ed.), Springer, Berlin. 1988, 186: 1–139.
[165] Chen Z.Y., Albright P.C., Sengers J.V., Crossover from singular critical to regular classical thermodynamic behavior of fluids. Physical Review A, 1990, 41: 3161–3177.
[166] Chen Z.Y., Abbaci A., Tang S., Sengers J.V., Global thermodynamic behavior of fluids in the critical region. Physical Review A, 1990, 42: 4470–4484.
[167] KIselev S.B., Ely J.F., Generalized crossover description of the thermodynamic and transport properties in pure fluids. Fluid Phase Equilibria, 2004, 222: 149–159.
[168] Kawasaki K., Kinetic equations and time correlation functions of critical fluctuations. Annals of Physics, 1970, 61(1): 1–56.
[169] Ferrell R.A., Decoupled-mode dynamical scaling theory of the binary-liquid phase transition. Physical Review Letters, 1970, 24: 1169–1172.
[170] Olchowy G.A., Sengers J.V., A simplified representation for the thermal conductivity of fluids in the critical region. International Journal of Thermophysics, 1989, 10: 417–426.
[171] Sengers J.V., Sengers J.M.H.L., Thermodynamic behavior of fluids near the critical point. Annual Review of Physical Chemistry, 1986, 37: 189–222.
[172] J. Rowlinson, F.L. Swinton, Liquids and liquid mixtures. 3rd ed., Butterworths, London, 1982.
[173] Gerasimov A.A., New generalized crossover equation of state in the wide range of the critical point. Bulleten of the Kaliningrad State University, 2003, 3: 30–37.
[174] Chialvo A.A., Cummings P.T. Solute induced effects on the structure and thermodynamics of infinitely dilute mixtures. American Institute of Chemical Engineering Journal, 1994, 40: 1558–1573.
[175] Cummings P.T., Chialvo A.A., Cochran H.D., Molecular simulation study of solvation structure in supercritical aqueous solutions. Chemical Engineering Science, 1994, 49: 2735–2748.
[176] Chialvo A.A., Cummings P.T., Comment on ‘Near critical phase behaviour of dilute mixtures’. Molecular Physics, 1995, 84: 41–48.
[177] Chialvo A.A., Fluctuation theory of mixtures. E. Matteoli, G.A. Manssori, (eds.), Taylor and Francis, New York, 1990, pp.: 131–209.
[178] Chialvo A.A., Determination of excess Gibbs free energy by the single-charging-integral approach. Infinite dilution activity coefficients and related quantities. The Journal of Physical Chemistry, 1991, 95: 6683–6687.
[179] Chialvo A.A., Cummings P.T., Encyclopedia of Computational Chemistry. Wiley, New York, 1998, pp. 2839–2859.
[180] O'Connell J.P., Sharygin A.V., Wood R.H., Infinite dilution partial molar volumes of aqueous solutes over wide ranges of conditions. Industrial & Engineering Chemistry Research, 1996, 35: 2808–2812.
[181] Eckert C.A., Ziger D.H., Johnston K.P., Ellison T.K., The use of partial molal volume data to evaluate equations of state for supercritical fluid mixtures. Fluid Phase Equilibria, 1983, 14: 167–175.
[182] Chimowitz E.H., Afrane G., Classical, non-classical critical divergences and partial molar properties from adsorption measurements in near-critical mixtures. Fluid Phase Equilibria, 1996, 120: 167–193.
[183] Wheeler J.C., Behavior of a solute near critical point of an almost pure solvent. Berichte der Bunsengesellschaft für Physikalische Chemie, 1972, 76: 308–318.
[184] Khazanova N.E., Sominskaya E.E., Partial molar volumes in the ethane-carbon dioxide systems near the critical points of the pure components. Russian Journal of Physical Chemistry, 1971, 45: 1485–1491.
[185] van Wasen U., Swaid I., Schneider G.M., Physico-chemical principles and applications of supercritical fluid chromatography (SFC). Angewandte Chemie International Edition in English, 1980, 19: 575–587.
[186] Fernández-Prini R., Japas M.L., Chemistry in near-critical fluid. Chemical Society Reviews, 1994, 23: 155–163.
[187] Harvey A.H., Levelt Sengers J.M.H., Correlation of aqueous Henry’s constant from 0°C to the critical point. American Institute Chemical Engineering Journal, 1990, 36: 539–546.
[188] Japas M.L., Levelt Sengers J.M.H., Gas solubility and Henry’s law near the solvent’s critical point. American Institute Chemical Engineering Journal, 1989, 35: 705–713.
[189] Harvey A.H., Supercritical solubility of solids from near-critical dilute – mixture theory. The Journal of Physical Chemistry, 1991, 94: 8403–8406.
[190] Furuya T., Teja A.S., Krichevskii parameters and the solubility of heavy n-alkanes in supercritical carbon dioxide. Industrial and Engineering Chemistry Research, 2000, 39: 4828–4830.
[191] Levelt Sengers J.M.H., Critical behavior of fluids: Concepts and applications. In: Supercritical Fluids:

Fundamentals for Applications, E. Kiran, J.M.H. Levelt Sengers, (eds.), Kluwer, Dordrecht, 1994, pp.: 3–38.

[192] Krichevskii I.R., Thermodynamics of critical phenomena in infinitely dilute binary solutions. Russian Journal of Physical Chemistry, 1967, 41: 1332–1338.

[193] Gude M.T., Teja A.S., The critical properties of dilute n-alkane mixtures. Molecular Physics, 1994, 81: 599–607.

[194] Bazaev A.R., Abdulagatov I.M., Bazaev E.A., Abdurashidova A., *p-v-T-x* measurements of {(1-x)H_2O+x C_2H_5OH} mixtures in the near-critical and supercritical regions. The Journal of Chemical Thermodynamics, 2007, 39: 385–411.

[195] Bazaev A.R., Abdulagatov I.M., Magee J.W., PVTx measurements for H_2O+D_2O mixtures in the near-critical and supercritical regions. Journal of Supercritical Fluids, 2003, 26: 115–128.

[196] Orakova S.I., Rasulov S.M., Abdulagatov I.M., Experimental study of the PVTx relationship, L- L-V and L-V phase boundary of n-Hexane + Water mixtures near the upper and lower critical lines. Physics and Chemistry of Liquids, 2014, 52: 130–198.

[197] Orakova S.I., Rasulov S.M., Abdulagatov I.M., Experimental study of the isomorphism behavior of weakly (C_{VX}) and strongly (C_{PX}, K_{TX}) singular properties of 0.082n-Hexane+0.918Water mixtures near the upper critical point. Journal of Molecular Liquids, 2013, 187: 7–19.

[198] Abdulagatov A.I., Stepanov G.V., Abdulagatov I.M., The critical properties of binary carbon dioxite containing mixtures. The Krichevskii parameter and related thermodynamic properties. Part II. Russian High Temperature, 2007, 45: 1–19.

[199] Abdulagatov A.I., Stepanov G.V., Abdulagatov I.M., Krichevskii parameter and thermodynamic properties of infinite dilute aqueous mixtures near the critical point of pure water. Russian Supercritical Fluids. Theory and Practice, 2007, 2: 20–54.

[200] Span R., Wagner W., A new equation of state for carbon dioxide covering the fluid region from the triple-point temperature to 1100 K at pressures up to 800 MPa. Journal of Physical and Chemical Reference Data, 1996, 25: 1509–1596.

[201] Abdulagatov A.I., Stepanov G.V., Abdulagatov I.M., The critical properties of a binary aqueous and CO_2 containing mixtures and the Krichevskii parameter. In: Supercritical Fluids. R. M. Belinsky, (ed.), Nova Science Publisher, Inc., New York, Chap. 2, 2010, pp.: 79–285.

[202] Sedlbauer J., O'Connell J.P., Wood R.H., A new equation of state for correlation and prediction of standard molal thermodynamic properties of aqueous species at high temperatures and pressures. Chemical Geology, 2000, 163: 43–63.

[203] Levelt Sengers J.M.H., Everhart C.M., Morrison G., Pitzer K.S., Thermodynamic anomalies in near-critical aqueous NaCl solutions. Chemical Engineering Communication, 1986, 47: 315–328.

[204] Morrison G., Correlation of partial molar volumes at infinite dilution of salts in water. Journal of Solution Chemistry 1988, 17: 887–901.

[205] Japas M.L., Fernandez-Pirini R., Horita J., Wesolowski D.J., Fractioning of isotopic species between coexisting liquid and vapor water: complete temperature range, including the asymptotic critical behavior. The Journal of Physical Chemistry, 1995, 99: 5171–5175.

[206] Fernandez-Prini R., Alvarez J.L., Harvey A.H., Aqueous solubility of volatile nonelectrolytes. In: Aqueous Systems at Elevated Temperatures and Pressures, 2004: 73–98.

[207] Plyasunov A.V., Shock E.L., Prediction of the vapor-liquid distribution constants for volatile onrlrctrolytes in water up to its critical temperature. Geochimca et Cosmochimica Acta, 2003, 67: 4981–5009.

[208] Alvarez J., Corti H.R., Fernandez-Prini R., Japas M.L., Distribution of solutes between coexisting steam and water. Geochimica et Cosmochimica Acta, 1994, 58: 2789–2798.

[209] Japas M.L., Alvarez J.L., Gutkowski K., Fernández-Prini R., Determination of the Krichevskii function in near-critical dilute solutions of I-2(s) and CHI3(s). The Journal of Chemical Thermodynamics, 1998, 30: 1603–1615.

[210] Mendez-Santiago J., Teja A.S., The solubility of solids in supercritical fluids. Fluid Phase Equilibria, 1999, 160: 501–510.

[211] Roth M., Krichevskii parameters of heavy n-alkanes in carbon dioxide: comparison of the results from solubility measurements and from supercritical fluid chromatography. Fluid Phase Equilibria, 2003, 212: 1–9.

[212] Furuya T., Teja A.S., The solubility of high molecular weight n-alkanes in supercritical carbon dioxide at pressures up to 50 MPa. Journal of Supercritical Fluids, 2004, 29: 231–236.

[213] McGuigan D.B., Monson P.A., Analysis of infinite dilution partial molar volumes using a distribution function theory. Fluid Phase Equilibria, 1990, 57: 227–247.

[214] O'Connell J.P., Thermodynamic properties of solutions based on correlation functions. Molecular Physics, 1971, 20: 27–33.

[215] Perry R.L., O'Connell J.P., Fluctuation thermodynamics properties of reactive components from species correlation function integrals. Molecular Physics, 1984, 52: 137–147.

[216] Abdulagatov A.I., Stepanov G.V., Abdulagatov I.M., Alisultanova G., Ramazanova A.E., Extrema of isochoric heat capacity of water and carbon dioxide. Chemical

Engineering Communications, 2003, 190: 1499–1520.

[217] Polikhronidi N.G., Abdulagatov I.M., Batyrova R.G., et. al., Experimental study of the isochoric heat capacity of diethyl ether (DEE) in the critical and supercritical regions. International Journal of Thermophysics, 2012, 33: 185–219.

[218] Gaddy E.M., White J.A., Experimental and linear-model behavior of $(\partial^2 P/\partial T^2)_V$ and $(\partial^2\mu/\partial T^2)_\rho$ near the critical point of carbon dioxide. Physical Review A, 1982, 26: 2218–2226.

[219] Stephenson J., Loci of maxima and minima of thermodynamic functions of a simple fluid. Canadian Journal of Physics, 1976, 54(12): 1282–1291

[220] Magee J.W., Kaboyashi R. Behavior of isochoric inflection loci. In: Proc. 8th Symposium on Thermophysical Properties, Thermophysical Properties of Fluids, J.V. Sengers, (ed.), ASME, New York. 1982,1: 321–325.

[221] Magee J.W., Thermophysical properties of natural refrigerants. In: The 20th Japan Symposium on Thermophysical Properties, Tokyo, 1999 October 20-22, p. 473-478.

[222] Magee J.W., Isochoric p-ϱ-T measurements on Difluoromethane (R32) from 142 to 396 K and pentafluoroethane (R125) from 178 to 398 K at pressures to 35 MPa. International Journal of Thermophysics, 1996, 17: 803–822.

[223] Theeuwes F., Bearman R.J., The p, V, T behavior of dense fluids IV. The p,V,T behavior of liquid xenon. The Journal of Chemical Thermodynamics, 1970, 2: 501–506.

[224] Bearman R.J., Theeuwes F., Bearman M.Y., Mandel F., Throop G.J., Equation of state of dense fluids. VII. PY theory of CV extrema and comparison with experiment. The Journal of Chemical Physics 1970, 52: 5486.

[225] Diller D.E., The specific heats (C_v) of dense simple fluids. Cryogenics, 1971, 11: 186–191.

[226] Gladun C., The specific heat at constant volume of liquid neon. Cryogenics, 1971, 4: 78-80.

[227] Guida R., Zinn-Justin S., Critical Exponents of the N-vector model. Journal of Physics A, 1998, 31: 8103–8121.

[228] Saul D.M., Wortis M., Jasnow D., Confluent singularities and the correction-to-scaling exponent for the d=3 fcc Ising model. Physical Review B, 1975, 11: 2571–2578.

[229] Fisher M.E., Orkoulas G., The Yang-Yang Anomaly in fluid criticality: experiment and scaling theory. Physical Review Letters, 2000, 85: 696–699.

[230] Cerdeiriña C.A., Orkoulas G., Fisher M.E. Soluble model fluids with complete scaling and yang-yang features. Physical Review Letters, 2016, 116(4): 040601.

[231] Orkoulas G., Fisher M.E., Ustun C., The Yang-Yang relation and the specific heats of propane and carbon dioxide. The Journal of Chemical Physics, 2000, 113: 7530–7545.

[232] Orkoulas G., Fisher M. E., Panagiotopoulos A.Z., Precise simulation of criticality in asymmetric fluids. Physical Review E, 2001, 63(5): 051507.

[233] Losada-Pérez P., Cerdeirina C.A., Coexisting densities and critical asymmetry between gas and liquid. The Journal of Chemical Thermodynamics, 2017, 109: 56–60.

[234] Barmatz M., Hohenberg P.C., Kornblit A., Scaled-equation-of-state analysis of the specific heat in fluids and magnets near critical point. Physical Review B, 1975, 12(5): 1947–1968.

[235] Hohenberg P.C. et al., Two-scale-factor universality and the renormalization group. Physical Review B, 1976, 13(7): 2986–2996.

[236] Stauffer D., Ferer M., Wortis M., Universality of second-order phase transitions: The scale factor for the correlation length. Physical Review Letters, 1972, 29(6): 345–354.

[237] Betts D.D., Guttmann A.J., Joyce G.S., Lattice-lattice scaling and the generalized law of corresponding states. Journal of Physics C: Solid State Physics, 1971, 4: 1994–2001.

[238] Abdulagatov I.M., Magee J.W., Polikhronidi N.G., Batyrova R.G., Yang-Yang critical anomaly. In: Enthalpy and Internal Energy: Liquids, Solutions and Vapors, T. Letcher, E. Wilhelm, Editors, Royal Society of Chemistry, 2017, Chapter 15, pp.380–410.

[239] Kiselev S.B., Kostyukova I.G., Povodyrev A.A., Universal crossover behavior of fluids and fluid mixtures in the critical region. International Journal of Thermophysics, 1991, 12(5): 877–895.

[240] Bagnuls C., Bervillier C., Nonasymptotic critical behavior from field theory at d= 3: The disordered-phase case. Physical Review B, 1985, 32(11): 7209–7231.

[241] Nieuwoudt J.C., et al., Transport properties of isobutane. Journal of Chemical and Engineering Data, 1987, 32: 1–8.

[242] Kiselev S.B., Kulikov V.D., Thermodynamic and transport properties of fluids and fluid mixtures in the extended critical region. International Journal of Thermophysics, 1997, 18(5): 1143–1182.

[243] Vesovic V., Wakeham W.A., Olchowy G.A., Sengers J.V., Watson J.T.R., Millat J., The transport properties of carbon dioxide. Journal of Physical and Chemical Reference Data, 1990, 19(3): 763–808.